Journal of
METAMORPHIC GEOLOGY

J. metamorphic Geol., 2017, **35,** 231–252 doi:10.1111/jmg.12230

Oxygen isotope thermometry using quartz inclusions in garnet

R. J. QUINN,[1,*] K. KITAJIMA,[1] D. NAKASHIMA,[1,2] M. J. SPICUZZA[1] AND J. W. VALLEY[1]
[1]*WiscSIMS, Department of Geoscience, University of Wisconsin, Madison, WI 53706, USA (ryanjoelquinn@gmail.com)*
[2]*Department of Earth and Planetary Material Sciences, Tohoku University, Aoba Sendai Miyagi 980-8578, Japan*

ABSTRACT Oxygen isotope ratios of quartz inclusions (QI) within garnet from granulite and amphibolite facies gneisses in the Adirondack Mountains, NY were analysed and used to determine metamorphic temperatures. Primary QI for eight of 12 samples have $\delta^{18}O$ values significantly lower than matrix quartz (MQ). The primary QI retain $\delta^{18}O$ values representative of thermal conditions during garnet crystallization, whereas the $\delta^{18}O$ values of MQ were raised by diffusive exchange with other matrix minerals (e.g. mica and feldspar) during cooling. The $\delta^{18}O$ differences between QI and MQ show that garnet (a mineral with slow diffusion of oxygen) can armour QI from isotopic exchange with surrounding matrix, even during slow cooling. These differences between $\delta^{18}O$ in MQ and QI can further be used to test cooling rates by Fast Grain Boundary diffusion modelling. Criteria for identifying QI that preserve primary compositions and are suitable for thermometry were developed based on comparative tests. Relations between $\delta^{18}O$ and inclusion size, distance of inclusion to host–garnet rim, core–rim zonation of individual inclusions, and presence or absence of petrological features (healed cracks in QI, inclusions in contact with garnet cracks lined by secondary minerals, and secondary minerals along the inclusion grain boundary) were investigated. In this study, 61% of QI preserve primary $\delta^{18}O$ and 39% were associated with features that were linked to reset $\delta^{18}O$ values. If $\delta^{18}O$ in garnet is homogeneous and inclusions are removed, laser-fluorination $\delta^{18}O$ values of bulk garnet are more precise, more accurate, and best for thermometry. Intragrain $\delta^{18}O(Grt)$ profiles measured *in situ* by ion microprobe show no $\delta^{18}O$ zonation. Almandine–rich garnet ($Alm_{60–75}$) from each sample was measured by laser-fluorination mass-spectrometry (LF-MS) for $\delta^{18}O$ and compared with ion microprobe measurements of $\delta^{18}O$ in QI for thermometry. The $\Delta^{18}O(Qz–Grt)$ values for Adirondack samples range from 2.66 to 3.24‰, corresponding to temperatures of 640–740 °C (A[Qz–Alm] = 2.71). Out of 12 samples that were used for thermometry, nine are consistent with previous estimates of peak temperature (625–800 °C) based on petrological and carbon–isotope thermometry for regional granulite and upper amphibolite facies metamorphism. The three samples that disagree with independent thermometry for peak metamorphism are from the anorthosite–mangerite–charnockite–granite suite in the central Adirondacks and yield temperatures of 640–665 °C, ~100 °C lower than previous estimates. These low temperatures could be interpreted as thermal conditions during late (post-peak) crystallization of garnet on the retrograde path.

Key words: ion microprobe; oxygen isotopes; quartz inclusions in garnet; speedometry; thermometry.

INTRODUCTION

Estimation of peak metamorphic temperatures using oxygen isotope fractionations among minerals has been widely applied over the past five decades (Garlick & Epstein, 1967; Bottinga & Javoy, 1975; Eiler *et al.*, 1993; Farquhar *et al.*, 1996; Valley, 2001; Larson & Sharp, 2005). Oxygen isotope thermometry records peak metamorphic conditions if two minerals attain equilibrium and are not modified during cooling and exhumation. However, the accuracy of $\delta^{18}O$ thermometry has been problematic for many systems due to retrograde exchange of oxygen between minerals or preservation of growth zoning (Deines, 1977; Edwards & Valley, 1988; Cartwright *et al.*, 1993; Eiler *et al.*, 1993, 1995; Kohn, 1999; Valley, 2001).

The Fast Grain Boundary (FGB) diffusion model (Eiler *et al.*, 1992, 1994) describes interdiffusion of stable isotopes between minerals in response to temperature changes; two primary assumptions are that equilibrium is maintained along grain boundaries and exchange occurs by diffusion in a closed system. This is distinct from Dodson's (1973) closure temperature because the FGB model links mass balance and diffusion for any number of minerals in a rock, whereas Dodson describes diffusion between a single mineral and an infinite reservoir. Dodson's closure temperature is a fixed temperature that is interpreted to mark the cessation of diffusion. In the FGB model, there is no assumption of a discrete closure temperature for any mineral; rather, a transition towards slower and slower diffusion is calculated where ultimately a

mineral no longer achieves measureable exchange and is effectively closed. Furthermore, because the FGB model accounts for mass-balance between all minerals in a rock, the mineralogical mode has a strong effect on exchange and resetting of $\delta^{18}O$.

The FGB model predicts that accurate temperatures can be obtained from a refractory accessory mineral within a matrix that is nearly monomineralic, but this approach is limited to specific rock types, including quartzites, marbles or anorthosites (RAM thermometry; Valley, 2001). In contrast, failure of the $\Delta^{18}O$(quartz–garnet, Qz–Grt) thermometer to record peak temperatures is predicted by the FGB model for many high-grade rocks with more diverse mineralogy due to diffusive exchange during cooling between quartz and other phases (e.g. feldspar and mica).

The prediction that matrix quartz (MQ) will reset is described by Figs 1 and 2, which demonstrate how MQ and biotite reset by diffusive exchange of oxygen during cooling. Such exchange renders the MQ and biotite problematic for thermometry studies of peak metamorphic conditions. However, if quartz is included within and armoured by a host mineral with slow oxygen diffusion such as garnet, then exchange for the inclusion is severely limited (barring recrystallization of the host mineral) and the quartz retains $\delta^{18}O$ values representative of peak conditions. The mineral inclusion–host method is similar to RAM thermometry in that the mineral with the lower closure temperature, for example, quartz, does not reset, but different in that the mechanism of peak $\delta^{18}O$(Qz) retention is armouring from oxygen exchange, rather than dilution.

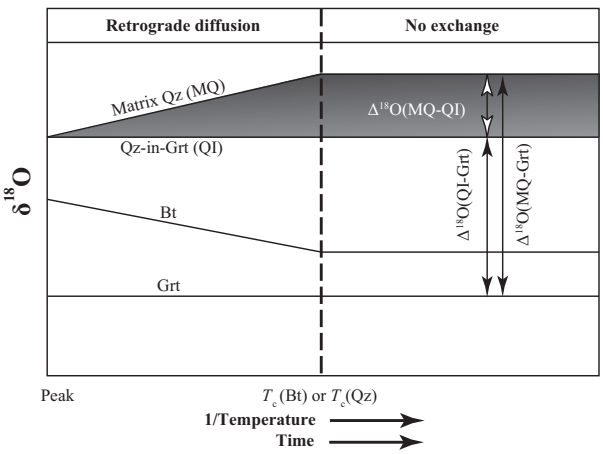

Fig. 1. Schematic progression of $\delta^{18}O$ values in the absence of fluids during cooling of a quartz (Qz) + biotite (Bt) + garnet (Grt) rock with quartz present in the matrix and as inclusions (QI) in garnet. Matrix quartz (MQ) and biotite exchange until the closure temperature of oxygen diffusion in either biotite or quartz (T_c (Bt) and T_c (Qz) are shown as equivalent for simplicity, vertical dotted line). Garnet is assumed to be closed to diffusion at peak temperature conditions and to armour quartz inclusions from exchange with matrix quartz and biotite. Arrows on the right side depict resulting $\delta^{18}O$ fractionations between MQ–Grt, QI–Grt and MQ–QI. Progression of $\Delta^{18}O$(MQ–QI) is highlighted by the shaded region.

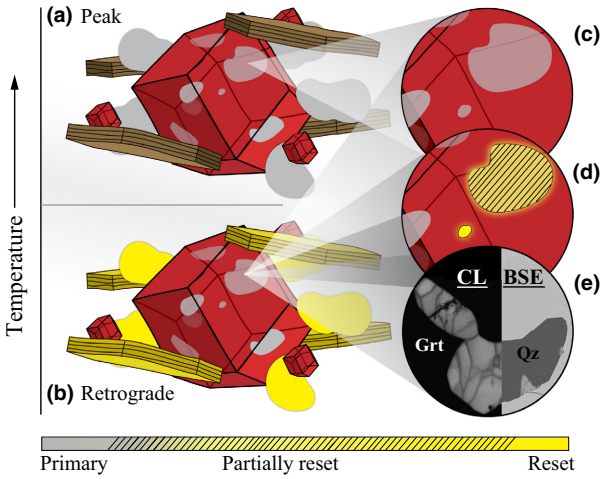

Fig. 2. Schematic diagram of a rock containing garnet (red), quartz (grey or yellow, rounded) and biotite (brown or yellow, tabular), and processes of oxygen isotope diffusion during retrograde metamorphism. The extent of resetting of $\delta^{18}O$ in quartz is shown by colour (scale at bottom). (a) At peak metamorphic temperatures, quartz inclusions in garnet are in equilibrium with matrix quartz and host garnet. (b) Retrograde oxygen exchange between matrix quartz and biotite causes reset $\delta^{18}O$ values for these minerals (yellow). (c) Below the closure temperature for garnet, primary quartz inclusions (PQI) preserve peak metamorphic $\delta^{18}O$ values. (d) If quartz inclusions and garnet hosts exchange oxygen by diffusion during cooling, smaller inclusions are more reset than larger inclusions and a diffusion profile in the garnet around the quartz inclusion is preserved. (e) Realistic complications: left – cathodoluminescence (CL) image of a quartz inclusion showing healed cracks, right – backscattered electron (BSE) image of a quartz inclusion showing secondary biotite along the inclusion–host grain boundary.

Quartz that is not armoured (e.g. MQ or quartz in garnet that is affected by fast pathways of exchange) can continue to exchange during cooling, leading to differences in $\delta^{18}O$ between armoured inclusions and MQ (Figs 1 & 2b) or inclusions that have leaked (Fig. 2e). Measureable differences between $\delta^{18}O$ in MQ and quartz inclusions (QI) are predicted for high-grade rocks that have crystallized above temperatures where oxygen readily diffuses in quartz and cooled slowly thereafter. Thermometry utilizing mineral inclusions could also be applicable to study of prograde metamorphism if spatially located in a mineral that preserves growth zoning of $\delta^{18}O$; such samples were not investigated in this study, but would make an interesting subject of future research.

Bulk analytical techniques have been unable to routinely investigate the stable isotope compositions of mineral inclusions due to their small size. Measuring stable isotope ratios of individual mineral inclusions and applying them to oxygen isotope

thermometry requires high-spatial–resolution and *in situ* analytical techniques. Improvement of ion microprobe (also called SIMS, secondary ion mass spectrometer) techniques has resulted in very precise analysis of ultra-small sample sizes (10 μm spot size, <1 ng of sample, 2SD = 0.3‰; Kita *et al*., 2009; Valley & Kita, 2009). Measurements of $\delta^{18}O$ in quartz are accurate and precise when compared to a homogeneous well-calibrated quartz standard (e.g. UWQ-1; Kelly *et al*., 2007). Measurements of $\delta^{18}O$ in garnet have improved with development of new garnet standards and analytical procedures over the past two decades (Hervig *et al*., 1992; Eiler *et al*., 1997; Vielzeuf *et al*., 2005a; Page *et al*., 2010; Kitajima *et al*., 2015). These improvements facilitate the investigation of oxygen isotope fractionations between mineral inclusions and their hosts.

The Qz–Grt pair is used in this study for several reasons. The Qz–Grt oxygen isotope thermometer is not measurably dependent on pressure (Clayton *et al*., 1975), and oxygen diffusion in garnet is slow (Coghlan, 1990), which promotes retention of peak $\delta^{18}O$ values. At equilibrium, quartz has the highest $\delta^{18}O$ of any mineral in a rock and garnet is sufficiently low in $\delta^{18}O$ such that the precision attainable for $\Delta^{18}O$(Qz–Grt) values allow for reasonably precise temperature estimates at high temperature (~ ±50 °C at 650–750 °C). Note that for SIMS data at high temperatures, this thermometer is not precise enough to test regional temperature gradients on the order of 100–150 °C. Larger $\Delta^{18}O$(Qz-mineral) values (i.e. more sensitive thermometers) are expected for magnetite ($\Delta^{18}O$(Qz–Mt) = 6.29 at 1000 K; Chiba *et al*., 1989) and rutile ($\Delta^{18}O$(Qz–Rt) = 3.66 at 1000 K; Valley *et al*., 2003), compared to garnet ($\Delta^{18}O$(Qz–Grt) = 2.71 at 1000 K; Coghlan, 1990). Magnetite and rutile are present in Adirondack rocks, but they suffer from orientation effects during ion microprobe analysis (Huberty *et al*., 2010; Kita *et al*., 2011; Taylor *et al*., 2012). Furthermore, magnetite often displays exsolved ilmenite, which suggests that $\delta^{18}O$(Mt) was altered by recrystallization or diffusion. Because of orientation effects during analysis and exsolution, magnetite and rutile are not appropriate for mineral-inclusion thermometry and thus garnet provides the largest equilibrium $\delta^{18}O$ fractionation with quartz.

We present $\delta^{18}O$ measurements of garnet, QI in garnet and MQ from granulite and upper amphibolite facies gneisses across the Adirondack Mountains, NY. These measurements are used to identify primary *v*. reset QI, evaluate the accuracy of $\Delta^{18}O$(QI–garnet) thermometry, and evaluate the effects of cooling rate and water fugacity on $\delta^{18}O$(MQ) values.

ADIRONDACK THERMOMETRY AND SPEEDOMETRY

The Adirondack Mountains, an outlier of the Grenville Province, are composed of the eastern Highlands

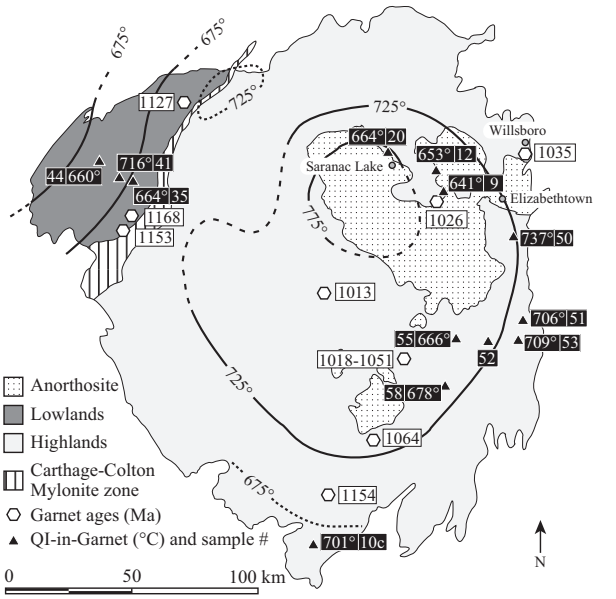

Fig. 3. Map of Precambrian rocks in the Adirondack Mts, NY showing concentric isotherms of peak temperature (°C; Kitchen & Valley, 1995). Isotherms are dashed where uncertain. Oxygen isotope thermometry estimates are based on fractionations between primary quartz inclusions (measured by ion microprobe) and host garnet (measured by laser-fluorination mass-spectrometry), with sample numbers (triangles; this study). Results of garnet geochronology (Basu *et al*., 1988; Mezger *et al*., 1991, 1992; Dewolf *et al*., 1996; Lapen *et al*., 2004; Connelly, 2006) are shown for reference (hexagons, Ma), but are not necessarily representative of garnet in this study, see text for discussion.

(granulite facies) and northwest Lowlands (upper amphibolite facies; Fig. 3). Bohlen *et al*. (1985) reviewed thermobarometric data for the Adirondacks and proposed a regional pattern of concentric peak temperature isotherms based mostly on estimates from magnetite–ilmenite and alkali feldspar–plagioclase thermometry with exsolved feldspar and oxides reintegrated, which are corroborated by phase equilibria and carbon–isotope thermometry in calc–silicates. Carbon–isotope results from calcite–graphite pairs are generally consistent with isotherm trends in the Highlands although locally temperatures are preserved from earlier events (Kitchen & Valley, 1995). The carbon isotope data represent a greater sampling density for the Lowlands area and provide the best estimate for isotherms in the Lowlands.

Data from Bohlen *et al*. (1985) and Kitchen & Valley (1995) indicate that peak metamorphic conditions are highest in the central Highlands (~800 °C and 7.5–8.0 kbar) and decrease radially (~640 °C and 6.0–6.5 kbar in the Lowlands; Fig. 3). This bull's eye pattern is centred about the exposed and presumed subsurface bodies of the Marcy Anorthosite massif and is proposed to have resulted from domical uplift of the isotherms. Despite common acceptance of the bull's eye isotherms (Fig. 3), many questions about

the accuracy and timing of regional thermometry remain in this complex polymetamorphic terrane. Estimates of ~850 °C have been reported in the western Highlands based on garnet–orthopyroxene and Ti-in-quartz thermometry (Darling *et al.*, 2004; Storm & Spear, 2009). In the southern Adirondacks, the 675 °C isotherm of Bohlen *et al.* (1985) is only constrained by one estimate of 660 °C. Other estimates in excess of 700 °C in this region suggest that peak temperatures were higher than indicated by the isotherm (Florence & Spear, 1995; Peck & Valley, 2004; Storm & Spear, 2005, 2009).

In the central highlands, two-pyroxene thermometry indicates peak metamorphic temperatures of 790–850 °C, but temperatures between Saranac Lake (above 775 °C isotherm) and Elizabethtown (below 725 °C isotherm; Fig. 3) are not significantly different within ±30 °C (Spear & Markussen, 1997). This suggests that different mineral systems record unique aspects of the *P–T* history or that some minerals are reset (e.g. Frost & Chacko, 1989). In addition, calibration errors could result in inconsistent temperatures between thermometers. Although there have been questions about the accuracy of temperature calibrations and effects of resetting for each of these thermometers, the general self-consistency and the widespread application of each thermometer across a large region supports the regional pattern as meaningful.

It was proposed that the intrusion of anorthosite–suite magmas predated the thermal peak of Ottawan granulite facies metamorphism and thus that evidence of multiple metamorphic events might be preserved (Valley & O'Neil, 1982). More recently, extensive geochronology in the Adirondacks has revealed three major periods of magmatism and associated high-grade metamorphism at 1168–1127, 1100–1054, and 1026–996 Ma (Mezger *et al.*, 1991; McLelland *et al.*, 1996, 2004, 2010; Wong *et al.*, 2012).

The thermometric evidence of poly-metamorphism has largely been erased by re-equilibration during the last phase of granulite metamorphism (Ottawan). Carbon isotope thermometry (Kitchen & Valley, 1995) records contact metamorphic temperatures in the cores of zoned graphite flakes from marbles adjacent to the *c.* 1150 Ma anorthosite massif, but most graphite in the region equilibrated at granulite facies conditions during the Ottawan *c.* 100 Ma later. Garnet $^{207}Pb/^{206}Pb$ ages of *c.* 1150 Ma are found in the southern Highlands and as young as *c.* 1030 Ma near the Marcy Anorthosite (Fig. 3; Mezger *et al.*, 1991). If garnet crystallized during multiple events, then $\Delta^{18}O$(Qz–Grt) thermometry could record multiple events as well. Furthermore, if different minerals represent different conditions within a single metamorphic episode, then discrepancy between thermometers (and between thermometry and chronology) could result. An example of this is described by Lancaster *et al.* (2009) who observed $\Delta^{18}O$(Grt–Zrc) disequilibrium during anatexis, along with rare-earth-element profiles across zircon that indicate zircon rims grew prior to the majority of garnet growth, and the Grt–Zrc pair in some migmatites never equilibrated with respect to $\delta^{18}O$.

Classically the Adirondacks have been viewed as a slowly cooled metamorphic terrane based on U–Pb ages of zircon, garnet, titanite, monazite and rutile; and Ar–Ar ages for hornblende and biotite (~1.5 °C Ma^{-1} in the Lowlands and 1–5 °C Ma^{-1} in the Highlands; Mezger *et al.*, 1991). This contrasts with cooling rate estimates for the Carthage–Colton shear zone (~25 km east of sample 44; Fig. 3) of 30–70 °C Ma^{-1} from ~675 to 500 °C based on intragrain zonation of $\delta^{18}O$ in titanite (Bonamici *et al.*, 2011, 2014, 2015). Contrasting cooling rates in the Lowlands and the Carthage–Colton shear zone can be explained by independent cooling histories, which could have resulted from northwest displacement of the Lowlands during exhumation of the Highlands along the Carthage–Colton shear zone (Mezger *et al.*, 1992; Streepey *et al.*, 2001; Johnson *et al.*, 2004; Selleck *et al.*, 2005; McLelland *et al.*, 2010). An *in situ* traverse from garnet from Willsboro reveals a 2.1‰ change in $\delta^{18}O$ over 16 μm, which suggest granulite facies metamorphism could only have lasted 1 Ma and that slow cooling would have further relaxed the diffusion profile (Page *et al.*, 2010). Bonamici *et al.* (2011, 2014, 2015) proposed a segmented cooling history where rapid changes on a time-scale of <50 Ma are followed by periods of slow cooling. A multi-stage cooling model is also proposed for the southern Highlands based on modelling of diffusion profiles in garnet and variably sized biotite inclusions in garnet (Storm & Spear, 2005), which yields a slow–fast–slow cooling history where slow periods cooling at ~8 °C Ma^{-1} and a fast period cooling at rates greater than 200 °C Ma^{-1} (Storm & Spear, 2005).

SAMPLE DESCRIPTIONS

A total of 59 hand samples were collected from 23 outcrops across the Adirondack Mountains based on the field identification of garnet and location with respect to the isotherms of Kitchen & Valley (1995). Thin-sections were made for all hand samples and examined using a polarizing microscope to identify samples with QI in garnet. Of the collected hand samples, 13 were selected for isotope analysis based on common occurrence of QI in garnet. Full sample names and locations are given in Table S1.

Samples #9 and 12 (meta-charnockite) and 20 (meta-granite) were collected from the anorthosite–mangerite–charnockite–granite suite (AMCG; emplacement *c.* 1155 Ma) in the central Adirondacks. Samples #35, 41 and 44 are paragneisses from the NW Lowlands. Five samples (#50, 51, 53, 55 and 58) were collected in the southeastern Adirondacks straddling the 725 °C isotherm (Fig. 3). Samples #50 and

53 are pelitic metasedimentary rocks and #51, 55 and 58 are orthogneisses. Two samples (#52 from Swede Pond and #10c from Irving Pond) were from thin section billets of feldspathic–garnetiferous quartzite previously described by Peck & Valley (2004) who analysed $\delta^{18}O$ in bulk quartz and garnet separates by laser-fluorination mass-spectrometry (LF-MS).

Garnet porphyroblasts from the 13 samples selected for isotope analysis range in diameter from 1 to 20 mm and contain QI ranging in size from μm's to hundreds of μm's (Figs 4 & 5). The abundance of QI in garnet varies between hand samples, but is consistent between garnet from the same hand sample. QI sometimes display healed cracks (HCs) in cathodoluminescence (CL; Fig. 5b,d,f) as well as open cracks (e.g., Fig. 5a), and some have variable amounts of secondary minerals along the host garnet – inclusion grain boundary (Fig. 5c,d). Many cracks

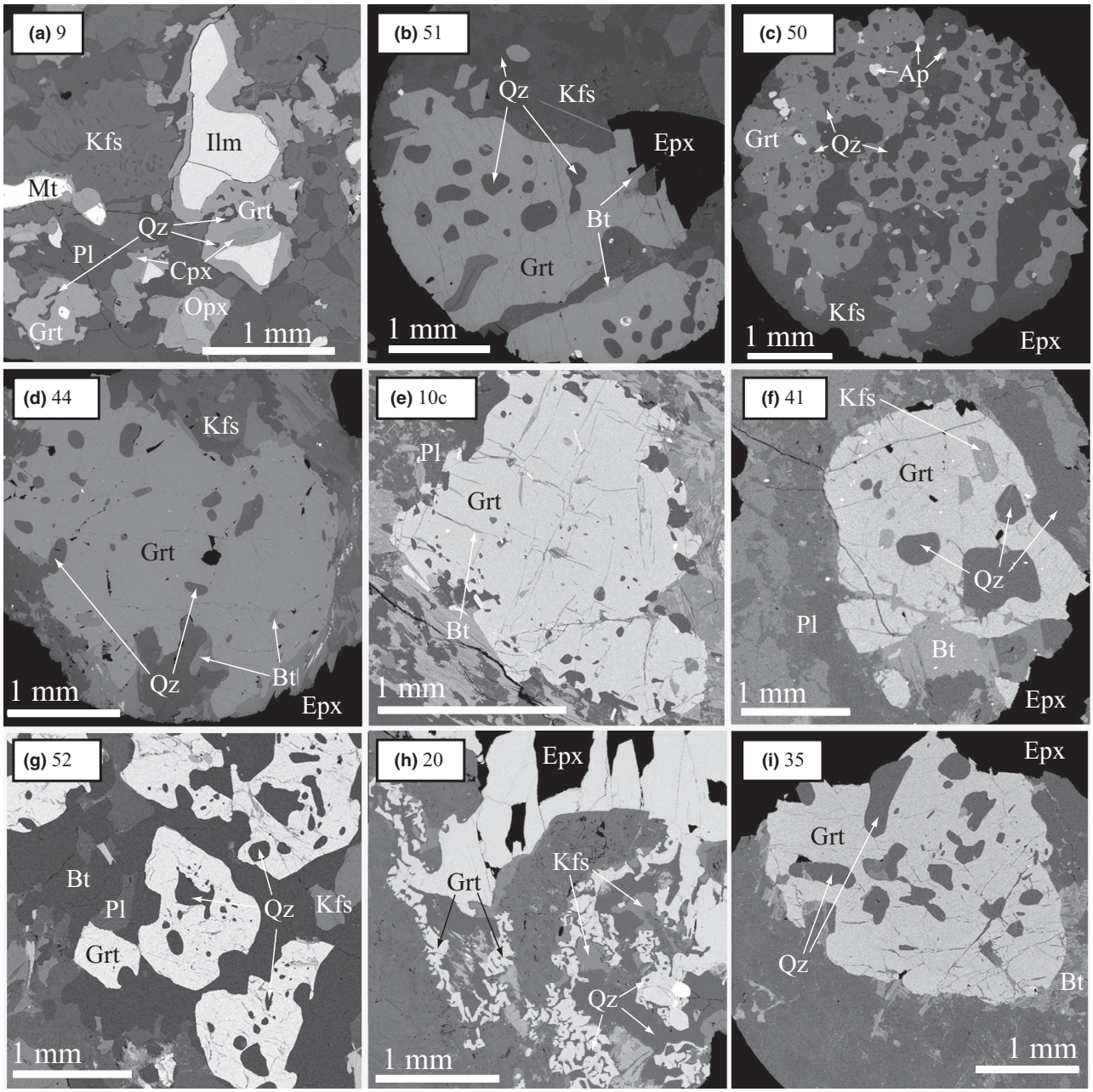

Fig. 4. Backscattered electron images of garnet with quartz inclusions. Sample numbers are given after figure labels. Ap, apatite; Bt, biotite; Cpx, clinopyroxene; Epx, epoxy; Grt, garnet; Ilm, ilmenite; Kfs, potassium feldspar; Mt, magnetite; Opx, orthopyroxene; Pl, plagioclase; and Qz, quartz.

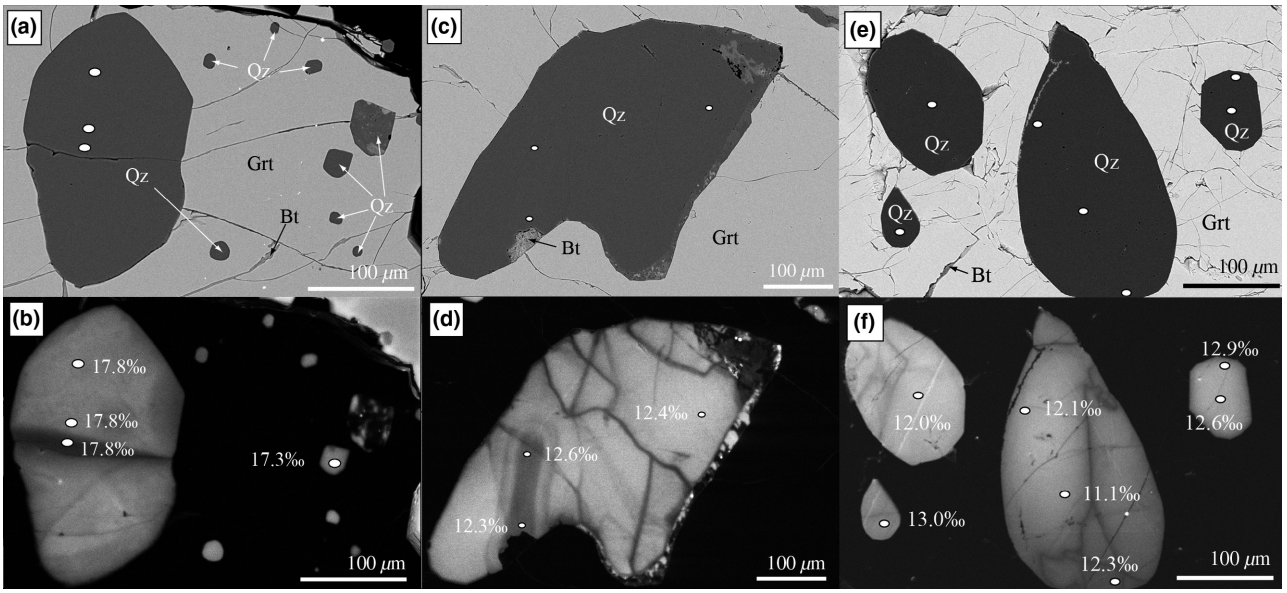

Figure 5. Backscattered electron (a), (c) and (e) and matching cathodoluminescence (b), (d) and (f) images of quartz inclusions in garnet. White ovals represent 10 μm diameter ion microprobe analysis pits. Oxygen isotope ratios are reported relative to VSMOW. Bt, biotite, Grt, garnet and Qz, quartz.

in the host garnet are lined with secondary biotite ± chlorite. These cracks commonly terminate at the host garnet – inclusion grain boundary but occasionally transect the inclusion (Figs 4 & 5). Such physical features could indicate communication between matrix phases and mineral inclusions in garnet at some time after the peak of metamorphism (e.g. Lamb *et al.*, 1987, 1991; Morrison & Valley, 1988; Whitney, 1996; Straume & Austrheim, 1999) and were evaluated for correlations with $\delta^{18}O$.

Garnet in sample #9 occurs as coronas <0.5 mm thick around ilmenite, clinopyroxene, and orthopyroxene and as porphyroblasts <2 mm in diameter (Fig. 4a). Garnet in samples #12 and 20 mostly form as porphyroblasts (diameters are ~2 mm in #12 and as large as 20 mm in #20), but also as vermicular Qz–Grt intergrowths (Fig. 4h). Garnet coronas and vermicular garnet were found exclusively in orthogneisses from the AMCG suite. QI were analysed for $\delta^{18}O$ from within the garnet coronas that surround ilmenite and pyroxene, within porphyroblasts and within the vermicular texture.

METHODS

Samples were mounted in epoxy, then ground and polished to prepare for scanning electron microscope (SEM) imaging, electron probe microanalysis (EPMA) and ion microprobe analysis. Imaging of samples by backscattered electrons (BSE) and CL was done to identify QI and textures critical to the interpretation of $\delta^{18}O$ data (Figs 4 & 5). Each ion microprobe analysis spot was chosen using the aid of SEM images. After $\delta^{18}O$ analysis, all ion microprobe pits were inspected by SEM to identify irregularities within the pit (similar to Cavosie *et al.*, 2005).

To correct for ion microprobe instrumental bias on $\delta^{18}O$(Grt) data, cation concentrations were determined adjacent to each pit using a CAMECA SX51 five-spectrometer electron microprobe at the University of Wisconsin–Madison. Garnet compositions were normalized to eight cations and Fe^{2+}/Fe^{3+} was calculated by charge balance (Valley *et al.*, 1983; Droop, 1987), which provides a good estimate of Fe^{2+}/Fe^{3+} in anhydrous garnet (Quinn *et al.*, 2016).

In situ $\delta^{18}O$ analyses were carried out using a CAMECA IMS 1280 at the WiscSIMS lab, University of Wisconsin–Madison under conditions similar to Kita *et al.* (2009). All oxygen isotope ratios are reported in standard ‰ notation relative to VSMOW. Raw $\delta^{18}O$(Qz) values were corrected for bias based on quartz standard UWQ-1 (Kelly *et al.*, 2007) analyses. Raw $\delta^{18}O$(Grt) values were corrected according to their mol.% grossular, almandine and spessartine (Kitajima *et al.*, 2015) based on eight garnet standards of varying composition (Fig. S1; Table S4).

If the oxygen isotopic composition of a garnet is shown to be homogeneous by ion microprobe analyses, then it can be advantageous to analyse a bulk garnet separate by LF-MS to obtain higher accuracy and reduce the propagated uncertainty in thermometry calculations. To reduce the possibility of contamination from mineral inclusions during LF-MS analysis of bulk garnet, a series of acid treatments was done to purify garnet in the analyte. To assess if

oxygen isotopes in garnet are fractionated during possibly incongruent dissolution of garnet in HF, inclusion–free garnet standard UWG-2 was acid treated and then analysed. No measurable difference in the $\delta^{18}O$ values was found between UWG-2 treated in HF for 0, 2, 4, 8 or 16 h, indicating that dissolution of almandine–rich garnet by 49% HF does not result in a measureable $\delta^{18}O$ fractionation (Table S5; 2SD = 0.1‰). Additional details for methods of sample preparation, SEM imaging, EPMA, ion microprobe analysis and LF-MS are provided in Appendix S1.

RESULTS

Criteria for primary Quartz Inclusions

Oxygen isotope ratios were analysed in 384 QI (430 spot analyses) within 57 garnet crystals from 13 samples. Values from these analyses range from 10.0 to 20.7‰ (Fig. 6; Table 2).

Numerous comparative tests were done to develop criteria for primary quartz inclusions (PQI) that are most suitable for thermometry calculations. These tests compared $\delta^{18}O$(QI) values to physical QI features, QI size, and QI location within the host garnet. All $\delta^{18}O$(QI), size and distance to garnet rim data are summarized in Table S6. Measurements of core and rim $\delta^{18}O$ data for QI were compared to determine if the QI are zoned and have reset.

Core and rim comparison of individual Quartz Inclusions

If garnet forms below the closure temperature of oxygen diffusion, no oxygen exchange between garnet and QI is expected, and both minerals should be homogenous in $\delta^{18}O$ (Fig. 2c). Numerous studies show that diffusion of oxygen in quartz is fast (Freer & Dennis, 1982; Dennis, 1984a,b; Giletti & Yund, 1984; Elphick *et al.*, 1986; Fortier & Giletti, 1989; Farver & Yund, 1991; Sharp *et al.*, 1991; Zheng & Fu, 1998) compared to garnet (Coghlan, 1990; Burton *et al.*, 1995; Russell *et al.*, 2013). If garnet and a QI exchanged oxygen, then a slight diffusion profile is predicted in the garnet, but the QI is expected to homogenize due to faster diffusion (Fig. 2d). Because a QI could reset and later homogenize, the absence of core–rim $\delta^{18}O$ zonation does not prove the fidelity of a QI. However, $\delta^{18}O$ zonation within individual QI provides unequivocal evidence that they have exchanged at lower temperatures along cracks in garnet and such quartz should not be used for thermometry. In addition, variability in $\delta^{18}O$ between QI indicates disequilibrium (if no growth zoning) and can be used as criteria for primary QI.

The difference in $\delta^{18}O$ between core and rim is more than 1‰ for three QI in sample #52, whereas all other samples is less than |0.5|‰ (Fig. 7); indicating some QI within #52 have been reset. Furthermore, $\delta^{18}O$(QI) values for all of the QI in this sample span a 4‰ range (Fig. 6) indicating disequilibrium between QI. The majority of QI in sample #52 is clearly not in equilibrium with garnet, and is not suitable for thermometry calculations. No other samples show $\Delta^{18}O$(core–rim) zonation for single QI.

Quartz Inclusions features

Several features identified by BSE and CL imaging suggest that some $\delta^{18}O$(QI) values are reset. Healed cracks are visible in some QI by CL imaging, but not by BSE imaging (e.g. Fig. 5). If HCs formed at high temperature, fluids were present and QI with HCs might be reset. It was also investigated whether spot $\delta^{18}O$ analyses of quartz on or off the HCs were different (e.g. Fig. 5b). If HCs were produced at a lower temperature where diffusion in quartz was not significant, the bulk QI could retain primary $\delta^{18}O$ values, whereas the quartz in HCs could have $\delta^{18}O$ different than the rest of the inclusion.

Cracks in host garnet (GC) are abundant and are often lined with secondary biotite or chlorite, indicating they formed at elevated temperature prior to final uplift and exposure (Fig. 5a,c,e). Healed cracks in garnet were not identified in this study. If garnet cracks extend from the QI–Grt grain boundary to the garnet–matrix grain boundary then exchange could occur with matrix minerals or fluids causing QI to become reset in $\delta^{18}O$. Secondary biotite and chlorite also occur along QI–Grt grain boundaries (Fig. 5c,d). The fluid required to precipitate secondary minerals could have exchanged oxygen with a QI.

The effect of each feature in QI was investigated *via* pairwise comparisons between average $\delta^{18}O$(QI) values (expressed as $\overline{QI}$) for each individual hand sample according to the following equations:

$$\Delta^{18}O(\overline{QI}_{[\text{healed cracks unobserved}]} - \overline{QI}_{[\text{healed cracks present}]}), \quad (1)$$

$$\Delta^{18}O(\overline{QI}_{[\text{off healed crack}]} - \overline{QI}_{[\text{on healed crack}]}) \text{ for QI with healed cracks present,} \quad (2)$$

$$\Delta^{18}O(\overline{QI}_{[\text{no observed connection with garnet crack}]} - \overline{QI}_{[\text{connected to garnet crack}]}), \text{ and} \quad (3)$$

$$\Delta^{18}O(\overline{QI}_{[\text{no observed secondary minerals}]} - \overline{QI}_{[\text{secondary minerals on QI}-\text{Grt garnet boundary}]}). \quad (4)$$

If the Eqns 1–4 are greater or less than zero by two standard errors (Fig. 8), then QI exhibiting the respective feature are referred to as non-primary quartz inclusions (nPQI; Table 2) and are not used for thermometry or $\Delta^{18}O$(MQ–QI) calculations. All other inclusions are referred to as PQI. Comparative tests between features are plotted for individual QI in Fig. S2. Testing the relationship between these

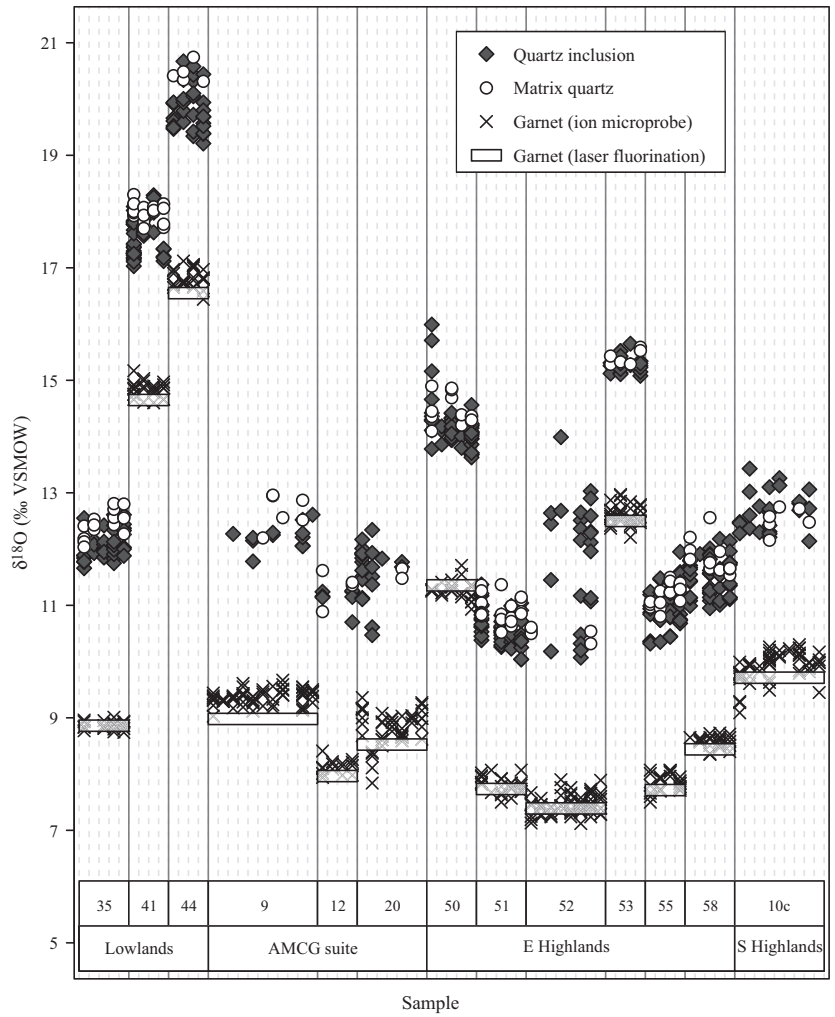

Fig. 6. Summary of $\delta^{18}O$ data for quartz inclusions (QI), matrix quartz (MQ), and garnet (Grt) by ion microprobe; and garnet by laser fluorination. The heights of the Grt laser–fluorination bars are 0.2‰ (2SD) centred about the average. The *X*-axis is grouped by hand sample (solid lines) and by individual garnet crystals (dashed lines). Matrix quartz data are associated with nearest garnet.

features and $\delta^{18}O$(QI) is limited to features observable by SEM; features above or below the plane of section could not be evaluated.

Healed cracks in quartz do not have a detectable effect on $\delta^{18}O$(QI), nor was a difference observed between spot measurements of $\delta^{18}O$(QI) on *v.* adjacent to HCs. This suggests that either (i) HCs in QI formed without causing a change in $\delta^{18}O$(QI) or that (ii) exchange occurred along a crack, the cracks subsequently healed and the QI was homogenized.

For QI where the QI–Grt interface is connected to garnet cracks, 11 of 13 samples show higher $\delta^{18}O$(QI) values (a negative $\Delta^{18}O$ value in Fig. 8c). Of all 13 samples with cracks in garnet, five have reset values where Eqn 2 is significantly less than zero. This indicates exchange along fast pathways can cause some QI to become reset.

Secondary mineral growth on QI grain boundaries represents retrograde metamorphism, but was associated with reset inclusions for two of 13 hand samples (#58 and 10c; Fig. 8d). Each hand sample likely has a distinct fluid history, which could explain the different results between hand samples.

Variation of $\delta^{18}O$(QI) from garnet core to rim

Values of $\delta^{18}O$(QI) were also compared to the minimum distance from the QI grain boundary to the host garnet rim to investigate possible 'zonation' of $\delta^{18}O$(QI) across the garnet host. Two samples (#41 and 58) show an apparent decrease in the variance of $\delta^{18}O$(QI) and a slight decrease in averaged $\delta^{18}O$(QI) from the garnet rim to core (Fig. 9e,k). This suggests that QI in these samples are more likely to be reset if closer to the garnet rim, even though some QI near the garnet rim were still armoured. However, the $\delta^{18}O$(QI) ranges in samples #41 and 58 are similar to other samples (~1‰), which suggests the $\delta^{18}O$(QI) is a homogenous population with random variability and the apparent trend is either fortuitous, or an artefact resulting from the 2D inspection of features summarized in Fig. 8 (i.e. a QI could be in contact with a crack in garnet below or above the polished surface and thus unseen). Other samples do not show any zonation or change in variance of $\delta^{18}O$(PQI) values with respect to distance from the garnet rim.

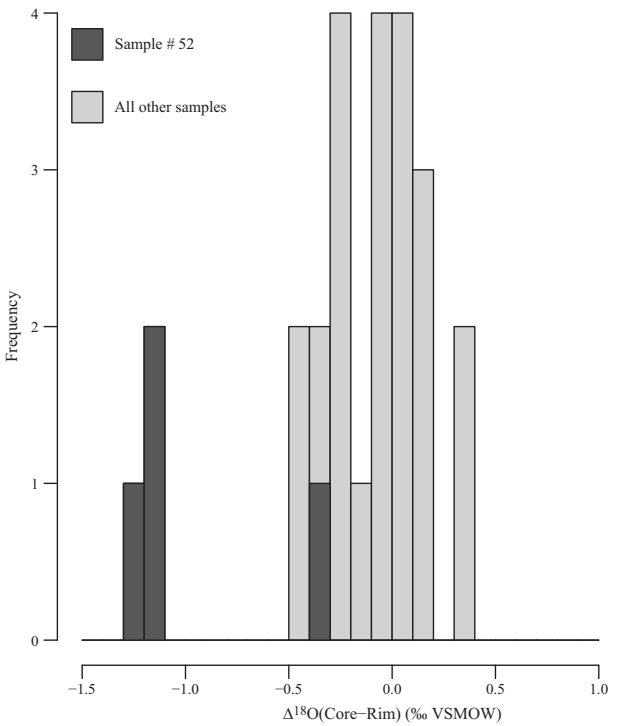

Fig. 7. Histogram of $\Delta^{18}O$(core–rim) values for individual quartz inclusions.

Size correlation test

Experimental estimates of the oxygen diffusion rate in garnet suggest slow diffusion ($D = 1.34 \times 10^{-25}$ m^2 s^{-1} at 750 °C; Coghlan, 1990). This is supported by empirical studies that indicate garnet is resistant to diffusional exchange at peak metamorphic temperatures in excess of 800 °C (Burton *et al.*, 1995; Wright *et al.*, 1995; Clechenko & Valley, 2003; Vielzeuf *et al.*, 2005b; Russell *et al.*, 2013). Furthermore, *in situ* analyses across a zoned garnet from the Willsboro wollastonite skarn (Fig. 3) reveals a 2.1‰ $\delta^{18}O$ gradient over a distance of 16 μm (Page *et al.*, 2010). Fitting a semi-infinite composite model to this gradient (eqns 3.45 and 3.46 in Crank, 1975) indicates the observed profile would form from a step gradient in < 1 Ma at 700 °C and thus could only be preserved through a shorter metamorphic event. Alternatively, if granulite facies metamorphism is longer or hotter, then oxygen diffusion in garnet is indicated to be slower than described by Coghlan (1990).

The possibility of oxygen exchange by diffusion between QI and host garnet was further investigated by calculating the diffusion distance of oxygen in garnet using eqn 2.45 of Crank (1975) for 1D diffusion in a semi-infinite medium. We use the diffusion data of Coghlan (1990) and a duration of 10 Ma at constant temperature. The result at 50% exchange is 65 μm at 800 °C, and 11 μm at 700 °C. These diffusion distances are large and would result in oxygen exchange between garnet and QI during cooling. These estimates are very conservative, considering the $\delta^{18}O$ gradient in the Willsboro garnet suggests that either metamorphism was shorter (<1 Ma) or diffusion is slower than proposed by Coghlan (1990), and present a case with the largest diffusion distance.

If diffusional exchange between garnet and QI is the only mechanism of exchange then the amount of resetting in the QI is fundamentally limited by the $\delta^{18}O$ equilibrium fractionation between quartz and garnet. The difference in equilibrium fractionation [$\Delta^{18}O$(Qz–Grt)] at 800 *v.* 700 °C is 0.51‰ (A(Qz–Grt) = 2.71, Valley *et al.*, 2003). Therefore, if garnet and QI were equilibrated at 800 °C, then cooled slowly to 700 °C, the maximum a QI would change is 0.51‰ (if garnet is the only exchange partner), which would occur for a very small inclusion. The minimum exchange for an infinitely large inclusion would be 0.0‰. All inclusions have finite size and are expected reset by ~0.1 to 0.5‰ depending on their size (assuming the Coghlan, 1990 diffusion rate accurately describes these samples). Differences in 0.5‰ could be measureable by ion microprobe, but not 0.1‰. If the same calculations were done for a system beginning in equilibrium at 800 °C that dropped to 600 °C and remained isothermal for 10 Ma, the maximum change in $\delta^{18}O$(QI) would be 1.2‰. However, diffusion in garnet is slow at 600 °C and exchange by diffusion would be severely limited.

To determine if small and large inclusions are measurably different in $\delta^{18}O$, a comparison was made of $\delta^{18}O$ for PQI ranging in size from 13 to 360 μm (minor-axis length in polished surface). No relation is observed between measured $\delta^{18}O$ values and PQI size (Fig. S3). However, the range of $\delta^{18}O$(PQI) for samples is ~1‰ thus differences of ≤0.5‰ may be obscured.

Matrix quartz

The ultimate test to determine if garnet armoured QI was to compare $\delta^{18}O$(PQI) to $\delta^{18}O$(MQ). A total of 133 $\delta^{18}O$ spot analyses of MQ were made, which range from 10.3 to 20.8‰ (Fig. 6). Eight of 12 samples with PQI have significant differences in $\delta^{18}O$ between MQ and QI ($\Delta^{18}O$(MQ–PQI) = 0.38–0.80‰; Table 2) indicating many of the QI in garnet were armoured from oxygen exchange.

Garnet

Ion microprobe

Ion microprobe measurements of $\delta^{18}O$(Grt) range from 6.4 to 16.9‰ for 447 analyses of 73 garnet grains (Fig. 6; Table S7). Garnet core and rim analyses were compared to determine if $\delta^{18}O$ zonation was present. No statistically significant trend in $\delta^{18}O$ is

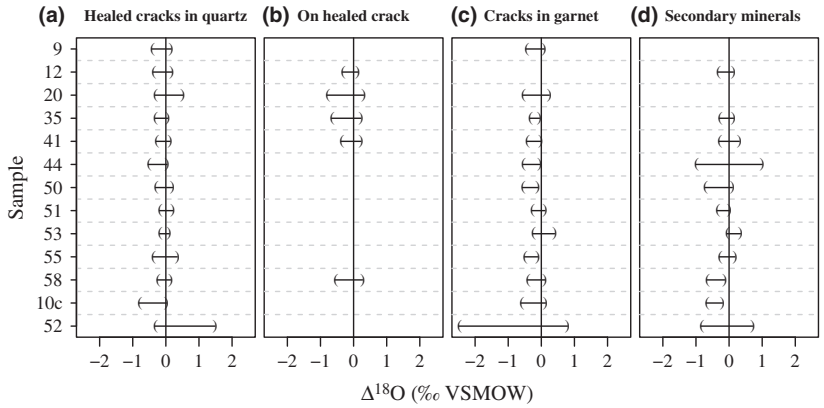

Fig. 8. Pairwise comparisons between quartz inclusions (QI) where physical features are either visible or unobserved by scanning electron microscopy. (a) $\Delta^{18}O$(QI with healed cracks visible – QI with healed cracks unobserved). (b) $\Delta^{18}O$(on healed crack – off healed crack) for QI where healed cracks are visible. (c) $\Delta^{18}O$(QI connected to cracks in garnet – QI not visibly connected to cracks in garnet). (d) $\Delta^{18}O$(secondary mineral growth visible along QI grain boundary – no observed secondary minerals along QI grain boundary). Error bars represent 2SE of the $\Delta^{18}O$ value. If the error bar does not overlap 0‰ (vertical solid black line) then QI's that display the feature were considered non-primary and were not used for thermometry calculations.

observed in any of the studied garnet (Fig. 10). Sample #10c has five spot analyses with low $\delta^{18}O$ values near the rim that are not in equilibrium with the core of the garnet. If these low $\delta^{18}O$(Grt) values near the rim are removed, the mean only changes by 0.07‰. If any low $\delta^{18}O$ portions of garnet from 10c were included in LF-MS analyses, it would not significantly reduce the bulk $\delta^{18}O$(Grt) value. Furthermore, for #10c, $\delta^{18}O$(QI) does not increase for QI near the host garnet rim (Fig. 9l), thus temperature calculations would not be significantly affected by any low $\delta^{18}O$(Grt) values near the rim. The homogenous $\delta^{18}O$(Grt) values for garnet by ion microprobe in this study indicate growth zones are not present and thus the variations in $\delta^{18}O$(QI) for samples #41 and 58 are not the result of growth zoning.

Cation chemistry

Analyses of cation concentrations by EPMA adjacent to $\delta^{18}O$ spots by ion microprobe reveal zonation patterns in Fe, Mg and Mn where cores are broad and generally homogeneous, with thin rims (<100 μm) where compositions vary. These patterns are interpreted as having formed during early retrograde conditions, consistent with Bohlen (1987). No characteristics of prograde zonation were observed. Each sub-region has some unique trends (Lowlands, central Highlands/AMCG, eastern Highlands, and southern Highlands; Appendix S2). The majority of samples from the eastern Highlands (#50, 51, 52, 55 and 58) are homogenous in Fe, Mg, Mn and Ca. One eastern Highlands sample (#53) shows increasing Ca and decreasing Mg towards the rim. Lowlands samples (#35, 41 and 44) display increasing Fe, Mn and Ca, and decreasing Mg towards the rim. Sample #10c from the southern Adirondacks is similar, but lacks Ca enrichment near the rims. In the AMCG–suite samples, cations in #9 are homogenous, whereas other samples (#12 and 20) show increasing Fe, Mg and Ca, and decreasing Mn towards the rim. Although some cation exchange has occurred, $\delta^{18}O$(Grt) is not detectably zoned (Fig. 10) and does not systematically change with garnet compositions (Appendix S2), thus cation zonation does not effect $\Delta^{18}O$(QI–Grt) thermometry.

Laser-fluorination mass-spectrometry

Laser-fluorination measurements of $\delta^{18}O$(Grt) range from 7.4 to 16.5‰ (Tables 1 & S5; Fig. 6) and are on average 0.16‰ lower than corresponding ion microprobe $\delta^{18}O$(Grt) data ($\Delta^{18}O$[ion microprobe - LF–MS] ranges from 0.39 to −0.09‰; Table 1). These values agree within analytical uncertainty for most samples, although $\delta^{18}O$(Grt) from LF-MS is systematically lower (slightly) than from ion microprobe. If quartz or feldspar inclusions were incorporated into the bulk garnet analysis, it would cause $\delta^{18}O$(Grt) measured by LF-MS to increase relative to $\delta^{18}O$(Grt) determined by ion microprobe, and thus incorporation of inclusions into LF-MS analysis of $\delta^{18}O$(Grt) does not explain the systematic offset between LF-MS and ion microprobe. Precision and accuracy of $\delta^{18}O$(Grt) data by LF-MS are better than by ion microprobe ($\sim\pm0.1$‰), and for homogeneous garnet, the LF-MS data are preferred.

DISCUSSION

Quartz–garnet thermometry

Samples where $\Delta^{18}O$(MQ–PQI) is significantly greater than 0.0‰ provide clear evidence that MQ can reset

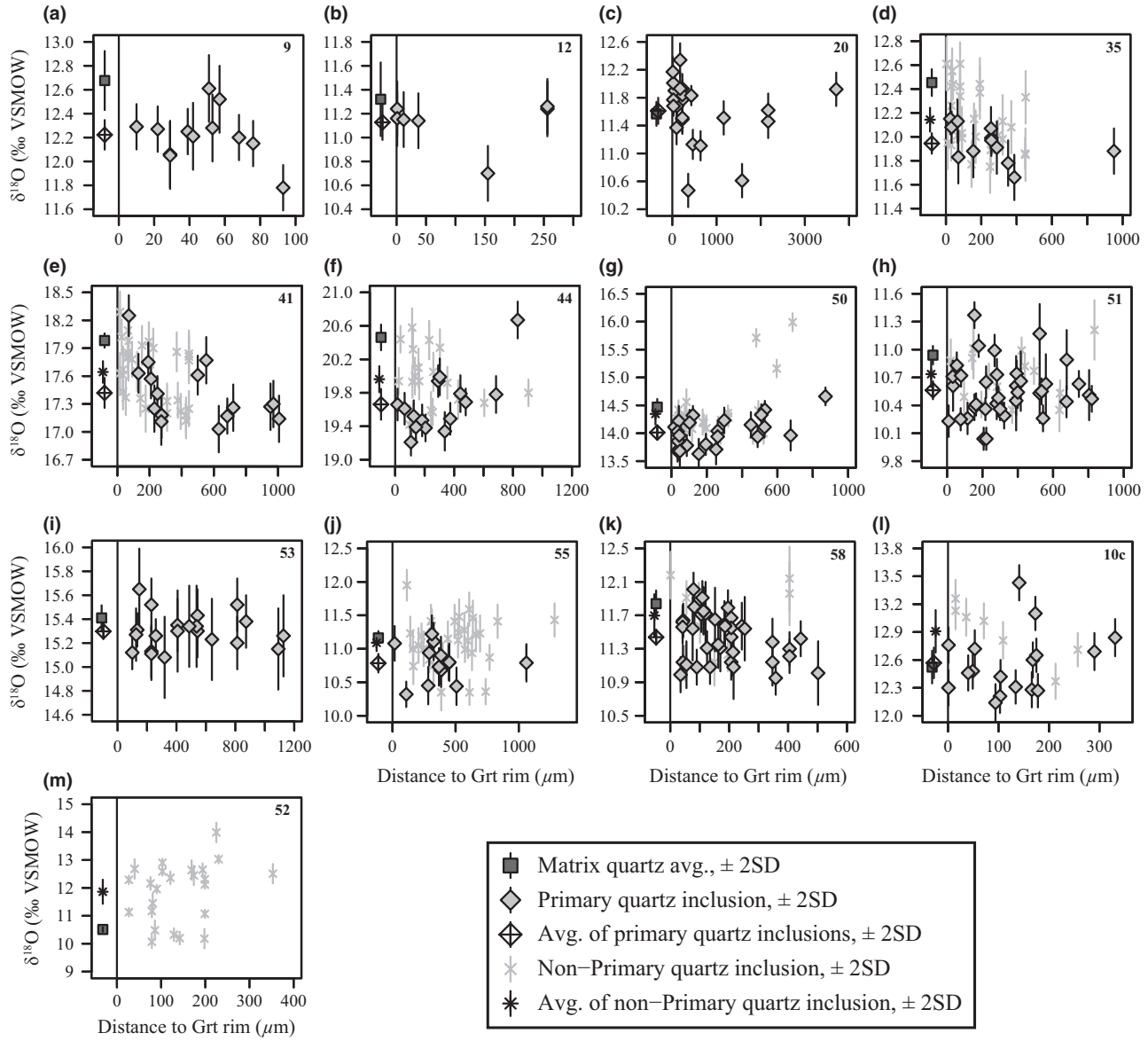

Fig. 9. Oxygen isotope data of quartz inclusions ±2SD and their distance from the garnet grain boundary with matrix minerals. Averages ±2SD of data for primary inclusions, non-primary inclusions, and matrix quartz are plotted for reference left of the solid line at $x = 0$.

and that QI can be armoured from processes that cause resetting of $\delta^{18}O$. For these samples, MQ is inappropriate for thermometry, but if instead PQI are employed, $\Delta^{18}O$ thermometry can work.

Oxygen isotope values of PQI can be applied to thermometry according to the relationship

$$\Delta^{18}O_{(Qz-Grt)} \approx 10^3 \ln[\alpha_{(Qz-Grt)}] = [A_{(Qz-Grt)} 10^6]/T^2, \quad (5)$$

where $\Delta^{18}O$(Qz–Grt) is the equilibrium fractionation between quartz and garnet, T is in K, α(Qz–Grt) is the fractionation factor, and the A-coefficient is equal to $\Delta^{18}O$ at 1000 K. Equation 5 assumes $\Delta^{18}O$(Qz-Grt) varies linearly *v.* $1/T^2$, which is common practice for mineral systems at temperatures above ~600 °C (Chacko *et al.*, 2001).

If garnet and QI preserve $\delta^{18}O$ values from the peak of metamorphism, then the largest uncertainty in oxygen isotope thermometry is the A(Qz–Grt) coefficient. For this study, an A(Qz–Grt) value of 2.71 $‰K^2$, determined empirically based on almandine-rich garnet (Valley *et al.*, 2003), is used for all temperature calculations. The A-value of 2.71 $‰K^2$ is expected to vary with certain cation substitutions in garnet; however, the effects from Fe^{2+} to Mg^{2+} between pure pyrope and almandine are negligible (Rosenbaum & Mattey, 1995). Similarly, effects from

Ca^{2+} to Mn^{2+} substitutions between pure grossular and spessartine are negligible (0–0.08‰) at 1000 K (Lichtenstein & Hoernes, 1992). Estimates of *A*(Alm–Grs) from 0.12 to 0.32 $‰K^2$ are retrieved if the *A* (Qz−[Alm + Prp]) = 2.71 $‰K^2$ value is combined with experimental (Matthews, 1994) and theoretical (Kieffer, 1982; Rosenbaum & Mattey, 1995) determinations of *A*(Qz–Grs). The effect of Ca^{2+} substitutions for Fe^{2+} and Mg^{2+} on *A*(Qz–Grt) is relatively small compared to the Fe^{3+}–Al^{3+} exchange, where Δ^{18}O(And-[Prp + Alm + Sps]) ranges from 0.45 to 0.70‰ at 1000 K (Kieffer, 1982; Rosenbaum & Mattey, 1995; Kohn & Valley, 1998).

Garnet compositions for this study have [Prp + Alm] from 72 to 96% [Grs + Sps] from 4 to 27%, and [And] <2% (Table 1). Linear interpolation between A-values for garnet compositions in this study result in *A*(Qz–Grt) values ranging from 2.72 to 2.80 $‰K^2$. Assuming A-values are correct, applying this linear interpolation to thermometry results in differences of ~0 to 10 °C *v.* temperatures calculated if *A*(Qz–Grt) = 2.71 $‰K^2$ for all garnet compositions.

Despite uncertainty in the fractionation calibration, any error in the *A*-coefficient would cause a systematic shift in all calculated temperatures (for homogeneous garnet) and thus relative differences observed between samples are precise. Remaining uncertainty in QI–Grt thermometry is due to instrumental precision and accuracy for ion microprobe δ^{18}O(Qz) and laser-fluorination δ^{18}O(Grt) measurements. Based on instrumental precision, the estimated precision for thermometry is ~40 to 80 °C.

Adirondack Lowlands

Average fractionations between primary QI and garnet for single rocks from the Lowlands range from

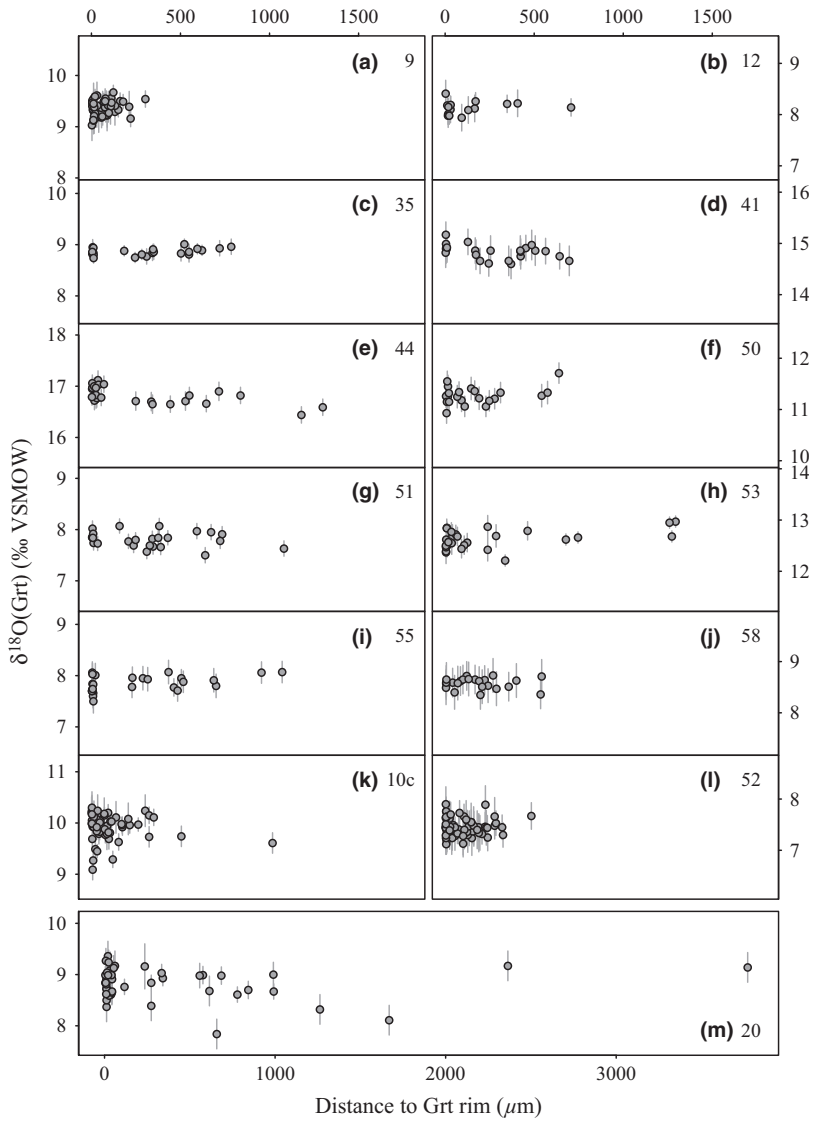

Fig. 10. Comparisons between oxygen isotope ratios of garnet and shortest distance of spot analysis from garnet grain boundary (μm) grouped by hand sample.

2.77 to 3.11‰, corresponding to temperatures ranging from 660 to 720 °C (Table 3; Figs 11 & 13). These temperatures are within 45 °C of $\Delta^{13}C$(calcite–graphite) thermometry (Kitchen & Valley, 1995) (Fig. 12). In contrast, $\Delta^{18}O$(MQ–Grt) values range from 3.33 to 3.91‰, corresponding to apparent temperatures of 560–630 °C (70–100 °C lower than $\Delta^{18}O$ (PQI–Grt) temperatures), and are not considered to represent equilibrium. These three Lowlands samples have the largest $\Delta^{18}O$(MQ–PQI) values ranging from 0.5 to 0.8‰ (Table 2; Fig. 11). This deviation between $\delta^{18}O$(MQ) and $\delta^{18}O$(PQI) is the result of garnet armouring QI from diffusion that resets $\delta^{18}O$ (MQ) during cooling.

Southern and Eastern Adirondack Highlands

Average fractionations between PQI and garnet for samples #10c, 50, 53, 55 and 58 range from 2.66 to 3.07‰ corresponding to temperatures of ~670 to 740 °C, which are within error of isotherms (Figs 3 & 12). The $\Delta^{18}O$(MQ–Grt) values do not represent equilibrium, and range from 2.81 to 3.45‰ corresponding to reset temperatures of ~610 to 710 °C (Table 3; Fig. 11).

Central Adirondack Highlands — AMCG suite

Samples from the AMCG suite yield the largest $\Delta^{18}O$ (QI–Grt) values of this study, ranging from 3.1 to 3.2‰ and correspond to the lowest temperatures of 640 to 665 °C (Table 3; Fig. 11). These temperatures are 100 to 200 °C lower than independent thermometry that shows the central Adirondacks as the highest temperature region (Fig. 3).

Values of $\Delta^{18}O$(MQ–QI) for these samples are −0.04, 0.19 and 0.46‰ (Table 2). The two values that are not significantly different than 0‰ (samples #12 and 20) suggest that the apparently reset $\Delta^{18}O$ (QI–Grt) values are the result of exchange between QI and matrix minerals during cooling, leading to reset temperatures. Furthermore, quartz within coronal and vermicular garnet might not truly be inclusions; the continuity of garnet coronas and vermiform in three dimensions is suspicious, and quartz within garnet coronas and vermiform are irregular compared to the equant QI in other samples (Fig. 4). The fidelity of QI from the AMCG samples in this study is thus questionable.

Another possible interpretation of the apparently reset temperatures for #9, 12 and 20 is that they represent temperatures of garnet crystallization during cooling. The $\Delta^{18}O$(MQ–QI) values of −0.04 and 0.19‰ could be explained by dry conditions resulting in arrested oxygen diffusion for all minerals, such that MQ does not reset compared to armoured QI. In contrast, #9 may have had a different fluid history where $f(H_2O)$ was sufficiently high for MQ to exchange with other matrix minerals, resulting in a larger $\Delta^{18}O$(MQ–QI) value of 0.45‰.

Timing and conditions of garnet growth in AMCG rocks have previously been discussed and debated with a focus on whether or not garnet grew at lower temperatures after the peak of metamorphism (de Waard, 1965; Buddington, 1966; Whitney & McLelland, 1973; McLelland & Whitney, 1977, 1980; Johnson & Essene, 1982; Whitney & McLelland 1983; Mezger *et al.*, 1991; Spear & Markussen, 1997). In particular, Gibbs-method modelling for Adirondack anorthosites (garnet+plagioclase+orthopyroxene+clinopyroxene+quartz) results in garnet necklaces between orthopyroxene and plagioclase growing from ~700 down to ~630 °C, if rocks cooled nearly isobarically (6 bar $°C^{-1}$ from 7 kbar) during post-Ottawan

Table 1. Garnet cation compositions and oxygen isotope values. Full data tables are reported in Table S7 (ion microprobe analyses of $\delta^{18}O$(Grt)), Table S3 (chronological $\delta^{18}O$ data for all quartz and garnet ion microprobe analyses), Table S5 (laser-fluorination mass-spectrometry $\delta^{18}O$ analysis of garnet), and Table S8 (electron microprobe analysis of garnet cation compositions).

		Average garnet composition (%)					Garnet composition (2SD)					Average $\delta^{18}O$(Grt) ‰			$\Delta^{18}O$ ‰
Sample	Rock type	Prp	Alm	Sps	Grs	And	Prp	Alm	Sps	Grs	And	Grt(SIMS)	2sd	Grt(LF)	(SIMS-LF)
Lowlands															
35	PHG	12	70	14	4	0	5.4	3.3	5.2	0.7	0.3	8.86	0.03	8.86	0.00
41	PHG	20	71	6	3	0	4.1	3.8	1.6	0.8	0.1	14.84	0.06	14.65	0.19
44	BtG	26	65	4	5	0	6.3	5.5	1.2	1.8	0.2	16.82	0.07	16.55	0.27
Highlands (AMCG)															
9	Chk	5	69	4	20	2	0.8	2.1	1.2	1.8	1.0	9.37	0.03	8.98	0.39
12	Chk	2	71	4	21	2	2.5	3.4	2.3	6.0	1.9	8.13	0.06	7.97	0.16
20	cgG	4	68	7	20	1	1.5	2.9	1.9	1.6	1.0	8.83	0.09	8.53	0.30
SE Highlands															
50	pG	30	61	2	7	0	1.8	2.6	0.9	1.7	0.4	11.27	0.07	11.36	−0.09
51	hgG	3	76	3	17	1	0.5	2.5	1.4	1.6	0.8	7.81	0.06	7.74	0.07
53	pG	28	66	2	4	0	1.2	2.4	1.1	0.6	0.2	12.62	0.07	12.50	0.12
55	hgG	3	71	3	22	1	0.5	2.4	1.1	1.8	1.2	7.85	0.06	7.72	0.13
58	gG	12	69	6	12	1	2.3	2.4	1.5	2.8	0.6	8.76	0.04	8.44	0.32
10c	Qtt	23	73	1	3	0	3.9	5.2	1.3	2.4	0.2	9.92	0.07	9.71	0.21
52	Qtt	16	76	3	5	0	1.1	2.5	1.1	0.8	0.3	7.45	0.04	7.39	0.06

Rock types: PHG, Popple Hill Gneiss; BtG, biotite gneiss; Chk, charnockite; cgG, clinopyroxene granitic gneiss; pG, pelitic gneiss; hgG, hornblende granitic gneiss; gG, granitic Gneiss; Qtt, quartzite.

cooling according to the reaction.

$$4\,\mathrm{Opx} + 4\,\mathrm{Pl} = 5\,\mathrm{Grt} + 1\,\mathrm{Cpx} + 1\,\mathrm{Qz} \qquad (6)$$

(Spear & Markussen, 1997).

Late crystallization of garnet at low temperature is consistent with a counter-clockwise *P–T* path and isobaric cooling after peak conditions. Numerous studies have presented evidence for isobaric cooling (Bohlen, 1987; Lamb *et al.*, 1991; Spear & Markussen, 1997; Storm & Spear, 2005), but a counter-clockwise path does not prove late crystallization. Furthermore, a clockwise *P–T* path is argued for by McLelland & Selleck (2011) who pointed out the cation zonation patterns discussed in Spear & Markussen (1997) could be the result of cooling after the igneous AMCG event at *c.* 1155 Ma.

If garnet crystallized prior to Ottawan metamorphism at *c.* 1090–1050 Ma, then the geochronology should pre-date *c.* 1050 Ma, whereas if garnet grew during isobaric cooling then it should have ages of 1050 Ma or younger. Some garnet grains have been dated from the Adirondack Highlands, but mostly from poly-metamorphic skarns, metasedimentary rocks and meta-gabbro at Gore Mountain (Fig. 3). Garnet ages from poly-metamorphic skarn garnet from Willsboro are 1035 Ma (Sm–Nd; Basu *et al.*, 1988), and garnet from the Cascade Slide xenolith is 1026 Ma (U/Pb; Mezger *et al.*, 1991; Dewolf *et al.*, 1996). Garnet at both Willsboro and Cascade Slide has a different mineralogy and history than AMCG rocks however, and should not be directly compared to samples in this study. Ages using the U/Pb method for three Highlands samples, a metagabbro (1013 Ma), a granitic gneiss (1064 Ma) and a paragneiss (1154 Ma), suggest different garnet grains record different metamorphic events spanning over 100 Ma (Mezger *et al.*, 1991). Igneous zircon in metagabbro from Dresden Station in the eastern Highlands is *c.* 1145 Ma; the metagabbro cross-cuts a metamorphic foliation associated with garnet, thus the garnet must pre-date 1145 Ma (McLelland & Chiarenzelli, 1989). Samples from Gore Mountain yield Lu–Hf ages ranging from 1047 to 1041 Ma (Lapen *et al.*, 2004; Connelly, 2006) and Sm–Nd ages from 1059 to 1018 Ma (Basu *et al.*, 1988; Mezger *et al.*, 1992). No geochronology yet exists for AMCG garnet. Detailed geochronology of AMCG garnet would answer the question of late crystallization and aid the interpretation of these low Δ^{18}O(PQI–Grt) temperatures.

Comparison of inclusions *v.* Matrix Quartz — Cooling Rate

If QI in garnet are armoured from oxygen diffusion, and MQ exchanges oxygen by diffusion with other matrix minerals during cooling, the δ^{18}O(MQ) value is predicted to be higher than δ^{18}O(PQI) within a

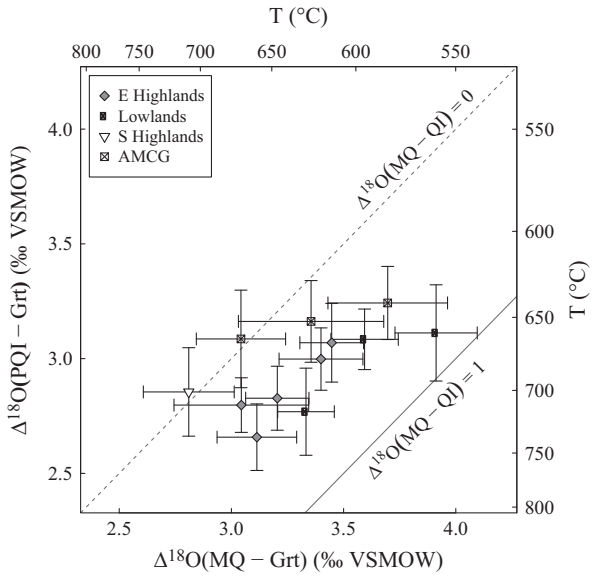

Fig. 11. Comparison of average values for oxygen isotope fractionations between matrix quartz (MQ) – garnet (Grt), and primary quartz inclusion (PQI) – Grt, grouped by hand sample. Quartz data are from ion microprobe analysis and garnet data are from laser–fluorination mass–spectrometry. Error bars are 2SE of measured Δ^{18}O (not estimated uncertainties of *T*). Temperature scales are calculated using *A* (Qz–Grt) = 2.71 (Valley *et al.*, 2003). Dashed line represents equilibrium between matrix quartz and quartz inclusions, that is, δ^{18}O(MQ) = δ^{18}O(PQI) and thus Δ^{18}O(PQI–Grt) – Δ^{18}O(MQ–Grt) = 0. Solid line represents δ^{18}O(PQI) = δ^{18}O(MQ) – 1 and thus Δ^{18}O(PQI–Grt) – Δ^{18}O(MQ–Grt) = −1. Sample #52 does not contain PQI and is not plotted, see text for discussion.

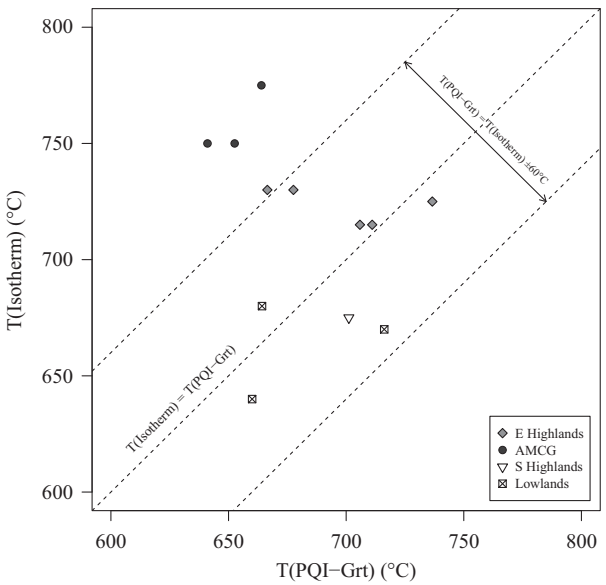

Fig. 12. Temperatures from δ^{18}O of pristine quartz inclusions (PQI; measured by ion microprobe) in garnet (Grt; measured by laser-fluorination mass-spectrometry) compared to isotherms (Fig. 3) for the peak temperatures of metamorphism (Kitchen & Valley, 1995). Data represent averages of hand samples.

Table 2. Results of pairwise comparisons between quartz inclusions with physical features observable or unobservable by scanning electron microscopy; and average oxygen isotope ratios for quartz inclusions and matrix quartz.

	Feature		Average $\delta^{18}O(Qz)$ ‰								Average $\Delta^{18}O$ ‰			
Sample	GC	SM	All QI	2SE	nPQI	2SE	PQI	2SE	MQ	2SE	(MQ-PQI)	2SE	(MQ-nPQI)	2SE
Lowlands														
35	nPQI	–	12.08	0.08	12.13	0.10	11.94	0.09	12.45	0.11	0.51	0.11	0.32	0.15
41	nPQI	–	17.57	0.10	17.64	0.12	17.42	0.16	17.98	0.08	0.56	0.18	0.34	0.14
44	nPQI	–	19.83	0.13	19.96	0.16	19.66	0.18	20.46	0.15	0.80	0.24	0.50	0.22
Highlands (AMCG)														
9	–	–	12.22	0.12	–	–	12.22	0.12	12.68	0.25	0.46	0.28	–	–
12	–	–	11.13	0.15	–	–	11.13	0.15	11.32	0.31	0.19	0.34	–	–
20	–	–	11.61	0.19	–	–	11.61	0.19	11.57	0.17	−0.04	0.25	–	–
SE Highlands														
50	nPQI	–	14.19	0.12	14.35	0.19	14.01	0.10	14.47	0.15	0.46	0.18	0.12	0.24
51	–	nPQI	10.61	0.08	10.94	0.14	10.56	0.10	10.94	0.10	0.38	0.14	0.00	0.17
53	–	–	15.30	0.06	–	–	15.30	0.06	15.54	0.11	0.25	0.29	–	–
55	nPQI	–	11.01	0.11	11.09	0.13	10.79	0.14	11.16	0.10	0.38	0.17	0.07	0.16
58	–	nPQI	11.49	0.09	11.70	0.25	11.44	0.09	11.84	0.16	0.40	0.18	0.14	0.30
10c	nPQI	nPQI	12.67	0.15	12.91	0.23	12.57	0.16	12.52	0.18	−0.04	0.24	−0.39	0.29
52[a]	–	–	11.86	0.43	11.86	0.43	–	–	10.51	0.08	–	–	−1.35	0.44

Healed cracks (HC); contact with garnet cracks (GC); secondary mineral growth (SM) along inclusion grain boundary; quartz inclusions (QI); non-pristine quartz inclusions (nPQI); pristine quartz inclusions (PQI); matrix quartz (MQ); anorthosite-mangerite-charnockite-granite (AMCG); and two standard errors (2SE).
[a]Although no physical features correlate with $\delta^{18}O(QI)$ values for sample 52; quartz inclusions from this sample are considered to all be non-primary based on the large $\delta^{18}O(QI)$ range (~4‰; Fig. 6) and $\Delta^{18}O$(core–rim) values of ~1‰ for individual quartz inclusions (Fig. 8).

closed system. This is because quartz has the highest $\delta^{18}O$ value compared to other minerals (assuming equilibrium) and thus any oxygen exchange between minerals during cooling would result in larger inter-mineral fractionations and an increase of $\delta^{18}O(MQ)$ values (e.g. Fig. 1). MQ from this study is typically higher in $\delta^{18}O$ compared to the associated primary QI (Fig. 6), and average measured $\delta^{18}O(PQI)$ values for eight of the 12 samples that contain PQI are significantly different than $\delta^{18}O(MQ)$ at 95% confidence. Three samples from the Lowlands have the largest $\Delta^{18}O(MQ–PQI)$ values ranging from 0.51 ± 0.11 to 0.80 ± 0.24‰, and are all significantly different than 0‰ (Table 2; Fig. 11). Nine samples from the Highlands range in $\Delta^{18}O(MQ–PQI)$ from -0.04 ± 0.24 to 0.46 ± 0.18‰, five of which are significantly >0.0‰.

Interpreting these differences between QI and MQ is aided by calculations using the FGB diffusion model (Eiler *et al.*, 1992, 1994). The FGB model calculates $\delta^{18}O$ of each mineral after cooling and for equilibrium at the initial temperature; for quartz, the initial $\delta^{18}O$ equilibrium is representative of primary QI and the final $\delta^{18}O$ is representative of MQ. Therefore, the difference between FGB calculations of $\delta^{18}O(Qz)$ at initial and final temperatures is a prediction of $\Delta^{18}O(MQ–PQI)$ in an actual rock.

A natural consequence of FGB calculations is that the diffusional resetting of MQ is proportional to the peak temperature and diffusion rate of oxygen; and inversely proportional to the ratio of oxygen in quartz/(mica+feldspar+oxides+quartz), grain size of MQ, and cooling rate. Petrographic microscopy can be used to estimate grain sizes and mineral proportions (Table S9). Inputs for temperature can be constrained by $\Delta^{18}O(PQI–Grt)$ or independent thermometry; $\Delta^{18}O(PQI–Grt)$ are used for all simulations described below. Numerous data sets exist that constrain diffusion rate of oxygen in minerals (reviewed by Farver, 2010), and fractionation factors have been estimated for many common minerals (reviewed by Chacko *et al.*, 2001). Diffusion and fractionation data for oxygen used as inputs are reported in Table S10. Once these parameters have been defined, the input value for cooling rate can be solved so that the FGB prediction for the amount MQ has reset (i.e. the predicted $\Delta^{18}O(MQ–PQI)$) agrees with the measured value of $\Delta^{18}O(MQ–PQI)$.

Table 3. Measured quartz–garnet oxygen isotope fractionations and calculated apparent temperatures for quartz inclusions in garnet and matrix quartz from the Adirondack Mountains; NY.

	Average $\Delta^{18}O$ ‰		Temperature (°C)[a]		
Sample	(PQI-Grt[b])	(MQ-Grt[b])	Isotherm	PQI-Grt[b]	MQ-Grt[b]
Lowlands					
35	3.08	3.59	680	664	595
41	2.77	3.33	670	716	629
44	3.11	3.91	640	660	559
Highlands (AMCG)					
9	3.24	3.70	750	641	583
12	3.16	3.36	750	653	626
20	3.09	3.04	775	664	671
SE Highlands					
50	2.66	3.11	725	737	660
51	2.83	3.20	715	706	646
53	2.80	3.04	715	711	670
55	3.07	3.45	730	666	614
58	3.00	3.40	730	678	620
10c	2.85	2.81	675	701	709
52[c]	–	3.12	725	–	659

[a]Temperatures calculated using the equation $\Delta^{18}O(Qz–Grt) = A(10^6/T^2)$; where $A(Qz–Grt) = 2.71$ (Valley *et al.*, 2003).
[b]Garnet values are based on laser-fluorination mass-spectrometry measurements.
[c]Quartz inclusions in sample 02AK52 are not in equilibrium (1‰ $\delta^{18}O$ zonation in single quartz inclusions and 4‰ $\delta^{18}O(QI)$ range for sample) and are generally not appropriate for thermometry.

The main uncertainty in estimating cooling rate in this manner derives from uncertainty in diffusion parameters. This is particularly true at lower temperatures where experimental data are extrapolated. Many estimates of the diffusion parameters for quartz exist including experimental (Freer & Dennis, 1982; Dennis, 1984a,b; Giletti & Yund, 1984; Elphick *et al*., 1986; Farver & Yund, 1991; Sharp *et al*., 1991), theoretical (Zheng & Fu, 1998) and empirical data (Fortier & Giletti, 1989). Diffusion rates in quartz have been shown to be dependent on $f(H_2O)$ (Dennis, 1984b; Giletti & Yund, 1984; Farver & Yund, 1991; Zhang *et al*., 1991), thus $f(H_2O)$ has significant effects on the outcome of isotopic compositions for a high-grade metamorphic rock during slow cooling (e.g. Edwards & Valley, 1988; Sharp *et al*., 1991; Kohn, 1999; Johnson *et al*., 2002; Peck & Valley, 2004). At high temperatures, retrograde fluid infiltration (Morrison & Valley, 1988) could alter the bulk $\delta^{18}O$ of a rock and change diffusion parameters due to changes in $f(H_2O)$ as demonstrated for magnetite (Valley & Graham, 1991, 1993) and diopside (Edwards & Valley, 1998) in Adirondack marbles. However, lower temperature infiltration, below the closure temperature of oxygen diffusion, would have no effect.

Case study: sample #44

The FGB model was used to investigate the effect $f(H_2O)$ and quartz polymorph (α- *v*. β-quartz), that is, diffusion rate, has on $\Delta^{18}O$(MQ–PQI). Sample #44, which is a biotite gneiss from the Lowlands is the best available sample to explore these effects because it has the largest measured $\Delta^{18}O$(MQ–PQI) value of $0.80 \pm 0.24‰$. A cooling rate of 1.5 °C Ma^{-1} was used (Mezger *et al*., 1991). Calculations were made using diffusion data for: dry β-quartz (Dennis, 1984b; Sharp *et al*., 1991), wet β-quartz (Elphick *et al*., 1986), and wet α-quartz (Farver & Yund, 1991) (Fig. 14). For a peak temperature of 660 °C, at pressures of ~6 kbar, SiO_2 in sample #44 would be α-quartz. Although β-quartz was not present for samples from the Lowlands (Fig. 3), it is useful to compare diffusion data for α and β-quartz as an example. No experiments for oxygen diffusion in dry α-quartz exist, although it is assumed dry α-quartz has slower diffusion than either wet α-quartz or dry β-quartz. Two sets of dry experiments are compared because data from Sharp *et al*. (1991) indicate diffusion is ~10 times faster compared to Dennis (1984b). The wet β-quartz diffusion data (Elphick *et al*., 1986) provide the fastest diffusion, and the dry β-quartz data (Dennis, 1984b) provide the slowest diffusion; together these two data sets describe upper and lower bounds of predicted $\Delta^{18}O$(MQ–PQI).

The best agreement between measured $\Delta^{18}O$(MQ–PQI) = 0.8‰, and predicted $\Delta^{18}O$(MQ–PQI) = 0.7‰ for a quartz grain of 1 mm radius results for sample #44, are achieved when wet diffusion data for α-quartz (Farver & Yund, 1991) are used (Fig. 14).

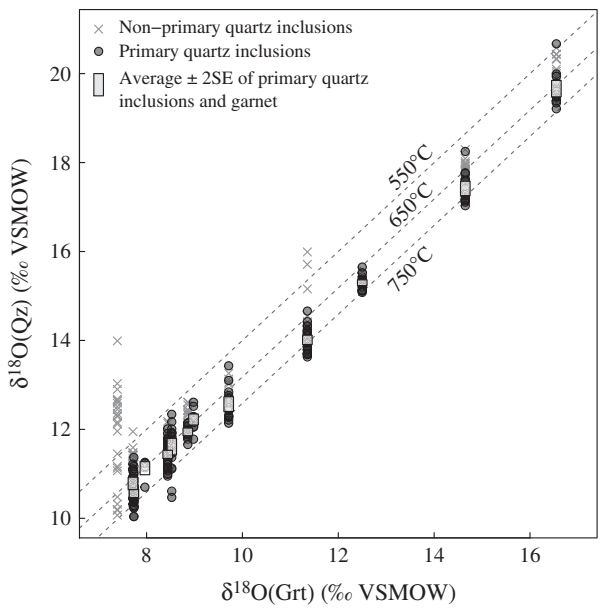

Fig. 13. Oxygen isotope ratios for primary and non-primary quartz (Qz) inclusions analysed by ion microprobe and garnet (Grt) analysed by laser fluorination. Rectangles show average values ±2SD about the $\delta^{18}O$ mean. Uncertainty for $\delta^{18}O$(Grt) is ±0.1‰. Isotherms were calculated using the equation $\Delta^{18}O$ [Qz–Grt] = $2.71(10^6/T^2)$ (Valley *et al*., 2003).

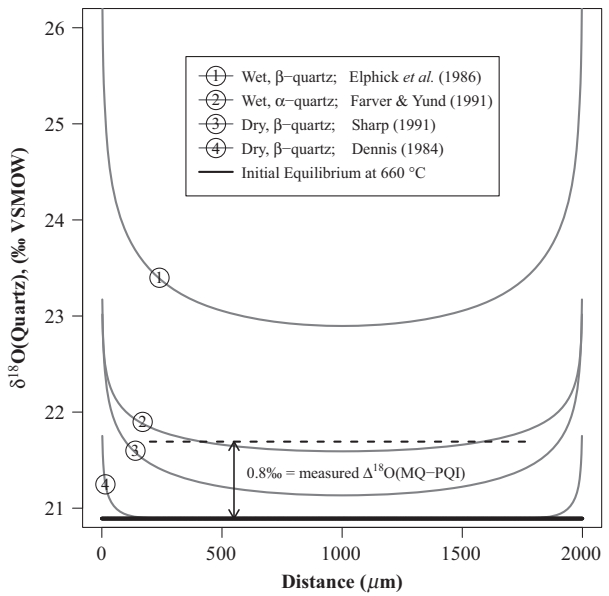

Fig. 14. Comparison of $\delta^{18}O$(Qz) results for sample #44 using various oxygen diffusion data, calculated using the Fast Grain Boundary model after cooling at 1.5 °C Ma^{-1} from 660 °C. The dashed line is plotted at 0.8‰ above the initial equilibrium to represent the measured $\delta^{18}O$ difference between matrix quartz (MQ) and primary quartz inclusions (PQI).

For samples from the Highlands (Fig. 3), SiO_2 may have existed as β-quartz at peak granulite facies conditions, but was certainly α-quartz for the majority of the retrograde path. Note that the distribution of $\delta^{18}O$ in quartz, calculated using the FGB model, is zoned. However, quartz would likely recrystallize during uplift, which would homogenize $\delta^{18}O$ in quartz as shown by in situ analysis. Thus, the measured $\Delta^{18}O$(MQ–PQI) values (dashed line; Fig. 14) should be an average and slightly higher than predicted $\Delta^{18}O$(MQ–PQI) values at the core.

Effects of mineral mode on $\delta^{18}O$(Qz) resetting

Another matter of interest is which minerals lead to the most change in $\delta^{18}O$(MQ) during cooling. Minerals that are in small modal abundance, or that have very slow oxygen diffusion (e.g. zircon, garnet or pyroxene) are expected to have a small or negligible effect on $\delta^{18}O$(MQ). Slow diffusion is important because if oxygen diffusion is effectively arrested in a mineral, that mineral will not exchange with quartz and thus not cause $\delta^{18}O$ resetting in quartz. A natural hypothesis is that minerals with higher closer temperatures will have less effect on $\delta^{18}O$ resetting of MQ. However, the fractionation between quartz and a mineral is ultimately what drives change in $\delta^{18}O$(MQ) during cooling. Oxygen diffusion in feldspar is faster than in biotite (Giletti *et al.*, 1978; Yund *et al.*, 1981; Fortier & Giletti, 1991), but the coefficients of A(quartz–plagioclase) = 1.26 and A(quartz–alkali feldspar) = 0.94 (Clayton *et al.*, 1989) are smaller than A(quartz–biotite) = 2.16 (calculated from quartz–calcite data, Clayton *et al.*, 1989; and phlogopite–calcite data, Chacko *et al.*, 1996). Magnetite has slower oxygen diffusion (Giletti & Hess, 1988) than mica or feldspar, but has a much larger A(quartz–magnetite) value of 6.29 (Chiba *et al.*, 1989).

Sample #44 has the smallest Qz/(Qz + Fsp + Mca + Mt) ratio, but which mineral is most responsible for quartz resetting ($\Delta^{18}O$(MQ–PQI) = 0.80‰)? Four simulations were ran using the FGB model where 72% of the mode (total of feldspar, biotite and magnetite) was comprised of only one mineral (biotite, plagioclase, alkali–feldspar or magnetite; Table S9) for each simulation. Radii for biotite, plagioclase, alkali–feldspar and magnetite were kept equal (1.5 mm) as a control. The biotite-rich sample resulted in the highest $\Delta^{18}O$(MQ–PQI) prediction equal to 1.1‰, whereas the magnetite rich sample resulted in the smallest $\Delta^{18}O$(MQ–PQI) prediction equal to 0.2‰ (for 1 mm radius quartz; Table S9). This test demonstrates that both diffusion rate and magnitude of fractionation are important factors that influence the resetting of quartz. Ultimately, the mineral that has the greatest effect on $\delta^{18}O$(MQ) resetting is dependent on the cooling history, and rock type.

Adirondack cooling rates

Fast Grain Boundary model calculations of $\Delta^{18}O$(MQ–PQI) were done for all samples using wet diffusion data for α-quartz (Farver & Yund, 1991) and a cooling rate of 1.5 °C Ma^{-1}. The predicted $\Delta^{18}O$(MQ–PQI) results are generally consistent with measured $\Delta^{18}O$(MQ–PQI) values (±0.3‰; Fig. 15). Comparison between Lowlands and Highlands samples suggests the Lowlands cooled more slowly than the Highlands. This is supported by the observations that (i) all Lowlands data plot on or below the 1:1 line, whereas all Highlands data plot above the 1:1 line (Fig. 15), and (ii) the Lowlands samples have the most reset $\delta^{18}O$(MQ) (Fig. 11; Table 2). One possibility is that the Lowlands were heated during the Ottawan orogeny to below peak-Shawinigan temperatures causing $\delta^{18}O$ values to reset in MQ, but not in more refractory minerals, e.g., garnet. Alternatively, if resetting of $\delta^{18}O$(MQ) was Shawinigan in age, then separate cooling histories for the Lowlands and Highlands would be expected as a result of unrelated metamorphic events.

Sample #10c displays the most disagreement between measured and predicted $\Delta^{18}O$(MQ–PQI) (Fig. 15). This sample is a quartzite, but is feldspathic (~28%) and micaceous (~15%; Qz/[Qz + Fsp + Mca + Mt] ≈ 0.54). Calculations using the FGB model predict that $\delta^{18}O$(MQ) should be reset

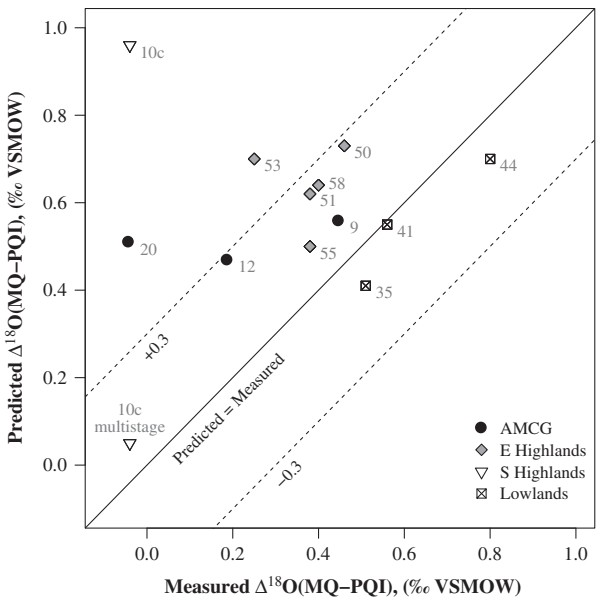

Fig. 15. Comparison between measurements and Fast Grain Boundary model calculations of differences between $\delta^{18}O$ of matrix quartz (MQ) and primary quartz inclusions (PQI) for quartz grains 1 mm in diameter. Samples are labelled adjacent to data points and are grouped by region. All Fast Grain Boundary simulations were conducted using $\Delta^{18}O$(PQI–Grt) thermometry results for peak temperatures; and a cooling rate of 1.5 °C Ma^{-1} except for the datum labelled '10c multistage', which incorporated a period of fast cooling (200 °C Ma^{-1}) between 650 and 450 °C.

during slow and wet cooling. There is no observed difference between $\delta^{18}O$(MQ) and $\delta^{18}O$(PQI) for #10c however, and the $\Delta^{18}O$(MQ–PQI) value of ~0.0‰ is more likely a result of fast cooling (e.g. Storm & Spear, 2005; Bonamici *et al.*, 2014) and/or low $f(H_2O)$ (e.g., Valley *et al.*, 1990; Peck & Valley, 2004). Predicted $\Delta^{18}O$(MQ–PQI) values for 10c are <0.01‰, if dry diffusion data are used (Dennis, 1984; Sharp *et al.*, 1991) even during slower cooling of 1.5 °C Ma^{-1} (Table S9), which is consistent with the observed value of -0.04 ± 0.25‰. A multistage cooling history proposed by Storm & Spear (2005) was tested with the FGB model by using a segmented cooling history that: (i) started at 700 °C, (ii) cooled to ~650 °C at 8 °C Ma^{-1}, (iii) cooled to 450 °C at a rate of 200 °C Ma^{-1}, then (iv) returned to cooling at a rate of 8 °C Ma^{-1} until 0 °C. The multistage simulation results in a predicted $\Delta^{18}O$(MQ–PQI) value of 0.05‰, also consistent with the observed value of -0.04 ± 0.25‰ (Fig. 15).

The predictions of FGB models implementing fast cooling, or multi-stage cooling incorporating periods of fast cooling, are ~0.0‰; even under hydrous conditions. Samples with significant differences between $\delta^{18}O$(MQ) and $\delta^{18}O$(PQI), both in the Highlands and the Lowlands, appear to be inconsistent with fast cooling from amphibolite and granulite temperatures. Samples with no significant $\delta^{18}O$ differences between MQ and primary QI, for example, sample #10c ($\Delta^{18}O$(MQ–PQI) = −0.04‰) can be explained using a fast cooling model. This contrast in $\Delta^{18}O$(MQ–PQI) values supports the conclusion of Bonamici *et al.* (2011, 2014, 2015) that locations where periods of rapid cooling occurred may be spatially limited.

CONCLUSIONS

Armoured QI and garnet hosts can be used to calculate peak temperatures (±50 °C). These temperatures are more accurate than conventional garnet–quartz thermometry for high-grade metamorphic rocks where MQ and garnet do not preserve equilibrium. Fractionations between garnet and MQ cannot be used for thermometry in rocks containing significant mica, feldspar or other exchangeable minerals because MQ will continue to exchange during cooling, resulting in disequilibrium between MQ and garnet. It is expected that $\delta^{18}O$(MQ) will be more disturbed in slow cooling terranes, and rocks with low modal proportions of Qz/(Qz + Mca + Fsp) in the matrix. Combining $\Delta^{18}O$(QI–Grt) thermometry and $\Delta^{18}O$(MQ–PQI) speedometry with garnet geochronology (Baxter & Scherer, 2013) and barometry using QI in garnet (Angel *et al.*, 2014; Ashley *et al.*, 2014; Kohn, 2014) would enable pressure, temperature, time and dT/dt information to be drawn from within a single garnet crystal. Combining such techniques provides a promising direction for future study of metamorphic domains.

ACKNOWLEDGEMENTS

We thank N. Kita, J. Kern and R. Kozdon for assistance in the WiscSIMS laboratory; B. Hess for thin section and epoxy mount preparation; J. Fournelle and P. Gopon for assistance with electron microprobe and scanning electron microscope; C. Bonamici for assistance with Fast Grain Boundary diffusion modeling; W. Peck for providing samples #10c and 52; W. Peck and two anonymous persons for helpful reviews; and M. Brown as editor. The majority of figures, data reduction, and calculations were done using R (R Core Team, 2013). This research was supported by the U.S. National Science Foundation (EAR-1144454 and EAR-1524336), by the US Department of Energy Office of Science, Office of Basic Energy Sciences, Chemical Sciences, Geosciences, and Biosciences Division under award number DE-FG02-93ER14389, and the University of Wisconsin-Madison Department of Geoscience. The WiscSIMS laboratory is partially supported by National Science Foundation (EAR-1355590).

REFERENCES

Angel, R.J., Mazzucchelli, M.L., Alvaro, M., Nimis, P. & Nestola, F., 2014. Geobarometry from host-inclusion systems: the role of elastic relaxation. *American Mineralogist*, **99,** 2146–2149.

Ashley, K.T., Caddick, M.J., Steele-MacInnis, M.J., Bodnar, R.J. & Dragovic, B., 2014. Geothermobarometric history of subduction recorded by quartz inclusions in garnet. *Geochemistry, Geophysics, Geosystems*, **15,** 350–360.

Basu, A., Faggert, B. & Sharma, M., 1988. Sm–Nd isotopic study of wollastonite skarn and garnet amphibolite metamorphism in the Adirondack Mountains, New York. *EOS*, **69,** 468.

Baxter, E.F. & Scherer, E.E., 2013. Garnet geochronology: timekeeper of tectonometamorphic processes. *Elements*, **9,** 433–438.

Bohlen, S.R., 1987. Pressure-temperature-time paths and a tectonic model for the evolution of granulites. *The Journal of Geology*, **95,** 617–632.

Bohlen, S.R., Valley, J.W. & Essene, E.J., 1985. Metamorphism in the Adirondacks I. Petrology, pressure and temperature. *Journal of Petrology*, **26,** 971–992.

Bonamici, C.E., Kozdon, R., Ushikubo, T. & Valley, J.W., 2011. High-resolution PTt paths from $\delta^{18}O$ zoning in titanite: a snapshot of late-orogenic collapse in the Grenville of New York. *Geology*, **39,** 959–962.

Bonamici, C.E., Kozdon, R., Ushikubo, T. & Valley, J.W., 2014. Intragrain oxygen isotope zoning in titanite by SIMS: cooling rates and fluid infiltration along the Carthage-Colton Mylonite Zone, Adirondack Mountains, NY, USA. *Journal of Metamorphic Geology*, **32,** 71–92.

Bonamici, C.E., Fanning, C.M., Kozdon, R., Fournelle, J.H. & Valley, J.W., 2015. Combined oxygen isotope and U-Pb zoning studies of titanite: new criteria for age preservation. *Chemical Geology*, **298,** 70–84.

Bottinga, Y. & Javoy, M., 1975. Oxygen isotope partitioning among minerals in igneous and metamorphic rocks. *Reviews of Geophysics*, **13,** 401–418.

Buddington, A., 1966. The occurrence of garnet in the granulite-facies terrane of the Adirondack highlands: a discussion. *Journal of Petrology*, **7,** 331–335.

Burton, K.W., Kohn, M.J., Cohen, A.S. & O'Nions, K.R., 1995. The relative diffusion of Pb, Nd, Sr and O in garnet. *Earth and Planetary Science Letters*, **133,** 199–211.

Cartwright, I., Valley, J.W. & Hazelwood, A.M., 1993. Resetting of oxybarometers and oxygen isotope ratios in granulite facies orthogneisses during cooling and shearing, Adirondack Mountains, New-York. *Contributions to Mineralogy and Petrology*, **113,** 208–225.

Cavosie, A., Valley, J. W. & Wilde, S. & E.I.M.F, 2005. Magmatic $\delta^{18}O$ in 4400–3900 Ma detrital zircons: a record of the alteration and recycling of crust in the Early Archean. *Earth and Planetary Science Letters*, **235,** 663–681.

Chacko, T., Hu, X., Mayeda, T.K., Clayton, R.N. & Goldsmith, J.R., 1996. Oxygen isotope fractionations in muscovite, phlogopite, and rutile. *Geochimica et Cosmochimica Acta*, **60,** 2595–2608.

Chacko, T., Cole, D.R. & Horita, J., 2001. Equilibrium oxygen, hydrogen and carbon isotope fractionation factors applicable to geologic systems. *Reviews in Mineralogy and Geochemistry*, **43,** 1–81.

Chiba, H., Chacko, T., Clayton, R.N. & Goldsmith, J.R., 1989. Oxygen isotope fractionations involving diopside, forsterite, magnetite, and calcite: application to geothermometry. *Geochimica et Cosmochimica Acta*, **53,** 2985–2995.

Clayton, R.N., Goldsmith, J.R., Karel, K.J., Mayeda, T.K. & Newton, R.P., 1975. Limits on the effect of pressure in isotopic fractionation. *Geochimica et Cosmochimica Acta*, **39,** 1197–1201.

Clayton, R.N., Goldsmith, J.R. & Mayeda, T.K., 1989. Oxygen isotope fractionation in quartz, albite, anorthite and calcite. *Geochimica et Cosmochimica Acta*, **53,** 725–733.

Clechenko, C.C. & Valley, J.W., 2003. Oscillatory zoning in garnet from the Willsboro Wollastonite Skarn, Adirondack Mts, New York: a record of shallow hydrothermal processes preserved in a granulite facies terrane. *Journal of Metamorphic Geology*, **21,** 771–784.

Coghlan, R. A. 1990. Studies in diffusional transport: Grain boundary transport of oxygen in feldspars, diffusion of oxygen, strontium, and the REE's in garnet, and the thermal histories of granitic intrusions in south-central Maine using oxygen isotopes. Unpublished PhD Thesis, Brown University, Providence, RI.

Connelly, J.N., 2006. Improved dissolution and chemical separation methods for Lu-Hf garnet chronometry. *Geochemistry, Geophysics, Geosystems*, **7,** 10.1029/2005GC001082.

Crank, J., 1975. *The Mathematics of Diffusion*. Oxford University Press, New York, NY, 414 pp.

Darling, R.S., Florence, F.P., Lester, G.W. & Whitney, P.R., 2004. Petrogenesis of prismatine-bearing metapelitic gneisses along the Moose River, west-central Adirondacks, New York. *Geological Society of America Memoir*, **197,** 325–336.

Deines, P., 1977. Oxygen isotope distribution among mineral triplets in igneous and metamorphic rocks. *Geochimica et Cosmochimica Acta*, **41,** 1709–1730.

Dennis, P.F., 1984a. Oxygen self-diffusion in quartz under hydrothermal conditions. *Journal of Geophysical Research*, **89,** 4047–4057.

Dennis, P.F., 1984b. Oxygen self diffusion in quartz. *Progress in Experimental Petrology, NERC Publication D*, **25,** 260–265.

Dewolf, C.P., Zeissler, C.J., Halliday, A.N., Mezger, K. & Essene, E.J., 1996. The role of inclusions in U-Pb and Sm-Nd garnet geochronology: stepwise dissolution experiments and trace uranium mapping by fission track analysis. *Geochimica et Cosmochimica Acta*, **60,** 121–134.

Dodson, M.H., 1973. Closure temperature in cooling geochronological and petrological systems. *Contributions to Mineralogy and Petrology*, **40,** 259–274.

Droop, G.T.R., 1987. A general equation for estimating Fe^{3+} concentrations in ferromagnesian silicates and oxides from microprobe analyses, using stoichiometric criteria. *Mineralogical Magazine*, **51,** 431–435.

Edwards, K.J. & Valley, J.W., 1998. Oxygen isotope diffusion and zoning in diopside: the importance of water fugacity during cooling. *Geochimica et Cosmochimica Acta*, **62,** 2265–2277.

Eiler, J.M., Baumgartner, L.P. & Valley, J.W., 1992. Intercrystalline stable isotope diffusion – a fast grain-boundary model. *Contributions to Mineralogy and Petrology*, **112,** 543–557.

Eiler, J.M., Valley, J.W. & Baumgartner, L.P., 1993. A new look at stable-isotope thermometry. *Geochimica et Cosmochimica Acta*, **57,** 2571–2583.

Eiler, J.M., Baumgartner, L.P. & Valley, J.W., 1994. Fast grain-boundary – a Fortran-77 program for calculating the effects of retrograde interdiffusion of stable isotopes. *Computers and Geosciences*, **20,** 1415–1434.

Eiler, J.M., Valley, J.W., Graham, C.M. & Baumgartner, L.P., 1995. Ion microprobe evidence for the mechanisms of stable-isotope retrogression in high-grade metamorphic rocks. *Contributions to Mineralogy and Petrology*, **118,** 365–378.

Eiler, J.M., Graham, C. & Valley, J.W., 1997. SIMS analysis of oxygen isotopes: matrix effects in complex minerals and glasses. *Chemical Geology*, **138,** 221–244.

Elphick, S., Dennis, P. & Graham, C., 1986. An experimental study of the diffusion of oxygen in quartz and albite using an overgrowth technique. *Contributions to Mineralogy and Petrology*, **92,** 322–330.

Farquhar, J., Chacko, T. & Ellis, D.J., 1996. Preservation of oxygen isotope compositions in granulites from Northwestern Canada and Enderby Land, Antarctica: implications for high-temperature isotopic thermometry. *Contributions to Mineralogy and Petrology*, **125,** 213–224.

Farver, J.R., 2010. Oxygen and hydrogen diffusion in minerals. *Reviews in Mineralogy and Geochemistry*, **72,** 447–507.

Farver, J.R. & Yund, R.A., 1991. Oxygen diffusion in quartz – dependence on temperature and water fugacity. *Chemical Geology*, **90,** 55–70.

Florence, F.P. & Spear, F.S., 1995. Intergranular diffusion kinetics of Fe and Mg during retrograde metamorphism of a pelitic gneiss from the Adirondack Mountains. *Earth and Planetary Science Letters*, **134,** 329–340.

Fortier, S.M. & Giletti, B.J., 1989. An empirical model for predicting diffusion coefficients in silicate minerals. *Science*, **245,** 1481–1484.

Fortier, S.M. & Giletti, B.J., 1991. Volume self-diffusion of oxygen in biotite, muscovite, and phlogopite micas. *Geochimica et Cosmochimica Acta*, **55,** 1319–1330.

Freer, R. & Dennis, P., 1982. Oxygen diffusion studies 1. A preliminary microprobe investigation of oxygen diffusion in some rock forming minerals. *Mineralogical Magazine*, **45,** 147–179.

Frost, B.R. & Chacko, T., 1989. The granulite uncertainty principle: limitations on thermobarometry in granulites. *The Journal of Geology*, **97,** 435–450.

Garlick, G.D. & Epstein, S., 1967. Oxygen isotope ratios in coexisting minerals of regionally metamorphosed rocks. *Geochimica et Cosmochimica Acta*, **31,** 181–214.

Giletti, B.J. & Hess, K.C., 1988. Oxygen diffusion in magnetite. *Earth and Planetary Science Letters*, **89,** 115–122.

Giletti, B. J. & Yund, R. A., 1984. Oxygen diffusion in quartz. *Journal of Geophysical Research: Solid Earth (1978–2012)*, **89,** 4039–4046.

Giletti, B., Semet, M. & Yund, R., 1978. Studies in diffusion—III. Oxygen in feldspars: an ion microprobe determination. *Geochimica et Cosmochimica Acta*, **42,** 45–57.

Hervig, R.L., Williams, P., Thomas, R.M., Schauer, S.N. & Steele, I.M., 1992. Microanalysis of oxygen isotopes in insulators by secondary ion mass spectrometry. *International Journal of Mass Spectrometry and Ion Processes*, **120,** 45–63.

Huberty, J.M., Kita, N.T., Kozdon, R. *et al.*, 2010. Crystal orientation effects on instrumental bias of $\delta^{18}O$ in magnetite by SIMS. *Chemical Geology*, **276,** 269–283. doi:10.1016/j.chemgeo.2010.06.012.

Johnson, C.A. & Essene, E.J., 1982. The formation of garnet in olivine-bearing metagabbros from the Adirondacks. *Contributions to Mineralogy and Petrology*, **81,** 240–251.

Johnson, E.A., Rossman, G.R., Dyar, M.D. & Valley, J.W., 2002. Correlation between OH concentration and oxygen

isotope diffusion rate in diopsides from the Adirondack Mountains, New York. *American Mineralogist*, **87,** 899–908.
Johnson, E.L., Goergen, E.T. & Fruchey, B.L., 2004. Right lateral oblique slip movements followed by post-Ottawan (1050–1020 Ma) orogenic collapse along the Carthage-Colton shear zone: data from the Dana Hill metagabbro body, Adirondack Mountains, New York. *Geological Society of America Memoirs*, **197,** 357–378.
Kelly, J.L., Fu, B., Kita, N.T. & Valley, J.W., 2007. Optically continuous silcrete quartz cements of the St. Peter Sandstone: high precision oxygen isotope analysis by ion microprobe. *Geochimica et Cosmochimica Acta*, **71,** 3812–3832.
Kieffer, S.W., 1982. Thermodynamics and lattice-vibrations of minerals: 5. Applications to phase-equilibria, isotopic fractionation, and high-pressure thermodynamic properties. *Reviews of Geophysics*, **20,** 827–849.
Kita, N.T., Ushikubo, T., Fu, B. & Valley, J.W., 2009. High precision SIMS oxygen isotope analysis and the effect of sample topography. *Chemical Geology*, **264,** 43–57.
Kita, N.T., Huberty, J.M., Kozdon, R., Beard, B.L. & Valley, J.W., 2011. High precision SIMS oxygen, sulfur and iron stable isotope analyses of geological materials: accuracy, surface topography and crystal orientation. *SIMS XVII Proceedings, Surface and Interface Analysis*, **43,** 427–431. doi:10.1002/sia.3424.
Kitajima, K., Strickland, A., Spicuzza, M. & Valley, J.W., 2015. Improvement in matrix correction of $\delta^{18}O$ analysis by SIMS for pyralspite and Cr-pyrope garnets. In: *Proceedings High – Resolution Proxies of Paleoclimate*, University of Wisconsin–Madison, May 31–June 3, p. 24.
Kitchen, N.E. & Valley, J.W., 1995. Carbon-Isotope thermometry in marbles of the Adirondack Mountains, New-York. *Journal of Metamorphic Geology*, **13,** 577–594.
Kohn, M.J., 1999. Why most "dry" rocks should cool "wet". *American Mineralogist*, **84,** 570–580.
Kohn, M.J., 2014. "Thermoba-Raman-try": calibration of spectroscopic barometers and thermometers for mineral inclusions. *Earth and Planetary Science Letters*, **388,** 187–196.
Kohn, M.J. & Valley, J.W., 1998. Effects of cation substitutions in garnet and pyroxene on equilibrium oxygen isotope fractionations. *Journal of Metamorphic Geology*, **16,** 625–639.
Lamb, W.M., Valley, J.W. & Brown, P.E., 1987. Post metamorphic CO_2-rich fluid inclusions in granulites. *Contributions to Mineralogy and Petrology*, **96,** 485–495.
Lamb, W.M., Brown, P.E. & Valley, J.W., 1991. Fluid inclusions in Adirondack granulites: implications for the retrograde PT path. *Contributions to Mineralogy and Petrology*, **107,** 472–483.
Lancaster, P.J., Fu, B., Page, F.Z. *et al.*, 2009. Genesis of metapelitic migmatites in the Adirondack Mountains, New York. *Journal of Metamorphic Geology*, **27,** 41–54.
Lapen, T.J., Mahlen, N.J., Johnson, C.M. & Beard, B.L., 2004. High precision Lu and Hf isotope analyses of both spiked and unspiked samples: a new approach. *Geochemistry, Geophysics, Geosystems*, **5,** 10.1029/2003GC000582.
Larson, T.E. & Sharp, Z.D., 2005. Interpreting prograde-growth histories of Al_2SiO_5 triple-point rocks using oxygen-isotope thermometry: an example from the Truchas Mountains, USA. *Journal of Metamorphic Geology*, **23,** 847–863.
Lichtenstein, U. & Hoernes, S., 1992. Oxygen isotope fractionation between grossular-spessartine garnet and water – an experimental investigation. *European Journal of Mineralogy*, **4,** 239–249.
Matthews, A., 1994. Oxygen-isotope geothermometers for metamorphic rocks. *Journal of Metamorphic Geology*, **12,** 211–219.
McLelland, J. & Chiarenzelli, J., 1989. Age of xenolith-bearing olivine metagabbro, eastern Adirondack Mountains, New York. *The Journal of Geology*, **97,** 373–376.
McLelland, J.M. & Selleck, B.W., 2011. Megacrystic Gore Mountain–type garnets in the Adirondack Highlands: age, origin, and tectonic implications. *Geosphere*, **7,** 1194–1208.
McLelland, J.M. & Whitney, P.R., 1977. The origin of garnet in the anorthosite-charnockite suite of the Adirondacks. *Contributions to Mineralogy and Petrology*, **60,** 161–181.
McLelland, J.M. & Whitney, P.R., 1980. Compositional controls on spinel clouding and garnet formation in plagioclase of olivine metagabbros, Adirondack Mountains, New York. *Contributions to Mineralogy and Petrology*, **73,** 243–251.
McLelland, J., Daly, J.S. & McLelland, J.M., 1996. The Grenville orogenic cycle (ca 1350–1000 Ma): an Adirondack perspective. *Tectonophysics*, **265,** 1–28.
McLelland, J.M., Bickford, M.E., Hill, B.M., Clechenko, C.C., Valley, J.W. & Hamilton, M.A., 2004. Direct dating of Adirondack massif anorthosite by U-Pb SHRIMP analysis of igneous zircons: implications for AMCG complexes. *Geological Society of America Bulletin*, **116,** 1299–1317.
McLelland, J.M., Selleck, B.W. & Bickford, M., 2010. Review of the Proterozoic evolution of the Grenville Province, its Adirondack outlier, and the Mesoproterozoic inliers of the Appalachians. *From Rodinia to Pangea: The Lithotectonic Record of the Appalachian Region: Geological Society of America Memoir*, **206,** 21–49.
Mezger, K., Rawnsley, C.M., Bohlen, S.R. & Hanson, G.N., 1991. U-Pb garnet, sphene, monazite, and rutile ages – implications for the duration of high-grade metamorphism and cooling histories, Adirondack Mts, New-York. *Journal of Geology*, **99,** 415–428.
Mezger, K., Essene, E.J. & Halliday, A., 1992. Closure temperatures of the Sm—Nd system in metamorphic garnets. *Earth and Planetary Science Letters*, **113,** 397–409.
Morrison, J. & Valley, J.W., 1988. Post-granulite facies fluid infiltration in the Adirondack Mountains. *Geology*, **16,** 513–516.
Page, F.Z., Kita, N.T. & Valley, J.W., 2010. Ion microprobe analysis of oxygen isotopes in garnets of complex chemistry. *Chemical Geology*, **270,** 9–19.
Peck, W.H. & Valley, J.W., 2004. Quartz-garnet isotope thermometry in the southern Adirondack Highlands (Grenville Province, New York). *Journal of Metamorphic Geology*, **22,** 763–773.
Quinn, R.J., Valley, J.W., Page, F.Z. & Fournelle, J.H., 2016. Accurate determination of ferric iron in garnets. *American Mineralogist*, **101,** 1704–1707.
R Core Team, 2013. *R: A Language and Environment for Statistical Computing*. R Foundation for Statistical Computing, Vienna, Austria. ISBN 3-900051-07-0, http://www.R-project.org/.
Rosenbaum, J.M. & Mattey, D., 1995. Equilibrium garnet-calcite oxygen-isotope fractionation. *Geochimica et Cosmochimica Acta*, **59,** 2839–2842.
Russell, A.K., Kitajima, K., Strickland, A., Medaris, L.G., Schulze, D.J. & Valley, J.W., 2013. Eclogite-facies fluid infiltration: constraints from $\delta^{18}O$ zoning in garnet. *Contributions to Mineralogy and Petrology*, **165,** 103–116.
Selleck, B.W., McLelland, J.M. & Bickford, M., 2005. Granite emplacement during tectonic exhumation: the Adirondack example. *Geology*, **33,** 781–784.
Sharp, Z., Giletti, B. & Yoder, H., 1991. Oxygen diffusion rates in quartz exchanged with CO_2. *Earth and Planetary Science Letters*, **107,** 339–348.
Spear, F.S. & Markussen, J.C., 1997. Mineral zoning, P-T-X-M phase relations, and metamorphic evolution of some Adirondack granulites, New York. *Journal of Petrology*, **38,** 757–783.
Storm, L.C. & Spear, F.S., 2005. Pressure, temperature and cooling rates of granulite facies migmatitic pelites from the southern Adirondack Highlands, New York. *Journal of Metamorphic Geology*, **23,** 107–130.
Storm, L.C. & Spear, F.S., 2009. Application of the titanium-in-quartz thermometer to pelitic migmatites from the Adirondack Highlands, New York. *Journal of Metamorphic Geology*, **27,** 479–494.

Straume, Å. & Austrheim, H., 1999. Importance of fracturing during retro-metamorphism of eclogites. *Journal of Metamorphic Geology*, **17,** 637–652.
Streepey, M., Johnson, E., Mezger, K. & van der Pluijm, B., 2001. Early history of the Carthage-Colton Shear Zone, Grenville Province, Northwest Adirondacks, New York (USA). *The Journal of Geology*, **109,** 479–492.
Taylor, R., Clark, C. & Reddy, S.M., 2012. The effect of grain orientation on secondary ion mass spectrometry (SIMS) analysis of rutile. *Chemical Geology*, **300,** 81–87.
Valley, J.W., 2001. Stable isotope thermometry at high temperatures. *Reviews in Mineralogy & Geochemistry*, **43,** 365–413.
Valley, J.W. & Graham, C.M., 1991. Ion microprobe analysis of oxygen isotope ratios in metamorphic magnetite-diffusion reequilibration and implications for thermal history. *Contributions to Mineralogy and Petrology*, **109,** 38–52.
Valley, J.W. & Graham, C.M., 1993. Cryptic grain-scale heterogeneity of oxygen isotope ratios in metamorphic magnetite. *Science*, **259,** 1729–1733.
Valley, J. & Kita, N., 2009. In situ oxygen isotope geochemistry by ion microprobe. *Mineralogical Association of Canada Short Course: Secondary Ion Mass Spectrometry in the Earth Sciences*, **41,** 19–63.
Valley, J.W. & O'Neil, J.R., 1982. Oxygen isotope evidence for shallow emplacement of Adirondack anorthosite. *Nature*, **300,** 497–500.
Valley, J., Essene, E. & Peacor, D., 1983. Fluorine-bearing garnets in Adirondack calc-silicates. *American Mineralogist*, **68,** 444–448.
Valley, J.W., Bohlen, S.R., Essene, E.J. & Lamb, W., 1990. Metamorphism in the Adirondacks. 2. The role of fluids. *Journal of Petrology*, **31,** 555–596.
Valley, J.W., Bindeman, I.N. & Peck, W.H., 2003. Empirical calibration of oxygen isotope fractionation in zircon. *Geochimica et Cosmochimica Acta*, **67,** 3257–3266.
Vielzeuf, D., Champenois, M., Valley, J.W., Brunet, F. & Devidal, J.L., 2005a. SIMS analyses of oxygen isotopes: matrix effects in Fe-Mg-Ca garnets. *Chemical Geology*, **223,** 208–226.
Vielzeuf, D., Veschambre, M. & Brunet, F., 2005b. Oxygen isotope heterogeneities and diffusion profile in composite metamorphic-magmatic garnets from the Pyrenees. *American Mineralogist*, **90,** 463–472.
de Waard, D., 1965. The occurrence of garnet in the granulite-facies terrane of the Adirondack Highlands. *Journal of Petrology*, **6,** 165–191.
Whitney, D.L., 1996. Garnets as open systems during regional metamorphism. *Geology*, **24,** 147–150.
Whitney, P.R. & McLelland, J.M., 1973. Origin of coronas in metagabbros of the Adirondack Mts, NY. *Contributions to Mineralogy and Petrology*, **39,** 81–98.
Whitney, P.R. & McLelland, J.M., 1983. Origin of biotite-hornblende-garnet coronas between oxides and plagioclase in olivine metagabbros, Adirondack region, New York. *Contributions to Mineralogy and Petrology*, **82,** 34–41.
Wong, M.S., Williams, M.L., McLelland, J.M., Jercinovik, M.J. & Kowalkoski, J., 2012. Late Ottawan extension in the eastern Adirondack Highlands: evidence from structural studies and zircon and monazite geochronology. *Geological Society of America Bulletin*, **124,** 857–869.
Wright, K., Freer, R. & Catlow, C.R.A., 1995. Oxygen diffusion in grossular and some geological implications. *American Mineralogist*, **80,** 1020–1025.
Yund, R., Smith, B. & Tullis, J., 1981. Dislocation-assisted diffusion of oxygen in albite. *Physics and Chemistry of Minerals*, **7,** 185–189.
Zhang, Y., Stolper, E. & Wasserburg, G., 1991. Diffusion of a multi-species component and its role in oxygen and water transport in silicates. *Earth and Planetary Science Letters*, **103,** 228–240.
Zheng, Y.F. & Fu, B., 1998. Estimation of oxygen diffusivity from anion porosity in minerals. *Geochemical Journal – Japan*, **32,** 71–90.

SUPPORTING INFORMATION

Additional Supporting Information may be found in the online version of this article at the publisher's web site:

Appendix S1. Methods.

Appendix S2. Cation compositions in garnet from EPMA analyses adjacent to ion microprobe pits; (left panel) per cent garnet end-member compositions compared to distance from garnet grain boundary and (right panel) comparison between end-member compositions in garnet and oxygen isotope ratios.

Figure S1. Step-wise matrix correction of garnet standards (Kitajima *et al.*, 2015) for two analytical sessions (4 – left panel; and 6 – right panel). (a) and (b) Bias relative to UWG-2 is fit to grossular mole per cent by a quadratic regression. (c) and (d) Residual bias after correcting for grossular is fit to spessartine mole per cent by a simple (straight line) regression. (e) and (f) Residual bias after correcting for grossular and spessartine is fit to almandine mole per cent by a quadratic regression. (g) and (h) Residual bias after correcting for grossular, spessartine, and almandine. Standards used for regressions are light blue diamonds and are: PypDM, R-53, and GrsSE for grossular regression; PrpDM and SpsSE for spessartine regression; and PypDM, UWG-2, and AlmSE for almandine correction (Table S4). Compositional ranges of studied garnet are highlighted by the grey field. Garnet end-member percents are defined as $[X/(Ca+Fe^{2+}+Mg+Mn)]^{*}100$; where X is Ca for grossular, Fe2+ for almandine, Mg for pyrope, and Mn for spessartine. Dashed lines represent best fit regressions. Solid lines are $y = 0$. Dotted lines in (g) and (h) are $y = \pm 0.3$.

Figure S2. Comparisons of quartz inclusion (QI) features: healed cracks (HC), on *v.* off healed cracks if healed cracks are visible (on/off HC), QI in contact with garnet cracks (GC), secondary mineral growth (SM) in QI and pristine inclusions. Columns one and three show all analyses by hand sample, columns two and four show the pairwise comparisons between average $\delta^{18}O$(QI) with feature present and average $\delta^{18}O$(QI) with feature unobserved ±2SE. Plots are grouped by sample.

Figure S3. Comparison between oxygen isotope values and size of primary quartz inclusions in garnet. Size is approximated by length of the minor axis (i.e. diameter; μm) as measured in the polished section.

Table S1. GPS coordinates for locations of samples (datum = NAD83).

Table S2. Ion microprobe data for all $\delta^{18}O$ analyses of quartz and garnet in chronological order from six analytical sessions.

Table S3. Electron probe microanalysis standards and conditions for analysis of major cations in garnet.

Table S4. Garnet standards for ion microprobe $\delta^{18}O$ analysis and their bias relative to UWG-2 for sessions 4 and 6 of this study.

Table S5. Oxygen isotope analyses of garnet by laser-fluorination and gas-source mass-spectrometry for Adirondack samples and HF tests on UWG-2.

Table S6. Ion microprobe $\delta^{18}O$ data for quartz inclusions with inclusion size, distance to garnet rim and inclusion core *v.* inclusion rim analyses.

Table S7. Oxygen isotope analyses of garnet by ion microprobe.

Table S8. Electron microprobe analysis of garnet major elements adjacent to ion microprobe pits.

Table S9. Fast Grain boundary model inputs and predictions of $\Delta^{18}O$ (matrix quartz – primary quartz inclusions).

Table S10. Fast grain boundary diffusion model inputs for oxygen diffusion parameters and geometries; oxygen isotope fractionation coefficients; and oxygen concentrations for each mineral.

Received 2 March 2016; revision accepted 22 October 2016.